NACA

RESEARCH MEMORANDUM

EFFECT OF FUEL DENSITY AND HEATING VALUE ON RAM-JET AIRPLANE RANGE

By Hugh M. Henneberry

Lewis Flight Propulsion Laboratory
Cleveland, Ohio

NATIONAL ADVISORY COMMITTEE
FOR AERONAUTICS

WASHINGTON

February 25, 1952

NATIONAL ADVISORY COMMITTEE FOR AERONAUTICS

RESEARCH MEMORANDUM

EFFECT OF FUEL DENSITY AND HEATING VALUE ON RAM-JET AIRPLANE RANGE

By Hugh M. Henneberry

SUMMARY

An analytical investigation of the effects of fuel density and heating value on the cruising range of a ram-jet airplane was made. In order to isolate fuel property effects as much as possible, the optimum compromise between weight and efficiency was approximated for the wing, engine, and fuselage. Fuel-property effects are presented for the optimum designs thus obtained. In addition, the effects of several design variables on ram-jet airplane cruising range are presented for an altitude of 70,000 feet and a Mach number of 3.5. The analysis included initial cruise altitudes from 35,332 to 100,000 feet, Mach numbers from 1.5 to 4.0, and fuel densities from 4 to 200 pounds per cubic foot. Results are based on an airplane initial gross weight of 150,000 pounds and a pay-load and controls weight of 10,000 pounds.

The results indicate that with present-day knowledge of chemical fuels, neither very high nor very low fuel densities have any advantages for long-range flight. Aircraft range was most sensitive to changes in fuel density at low altitudes and high Mach numbers and the best initial cruise conditions for maximum range were between altitudes of 50,000 and 70,000 feet and Mach numbers of 3.0 and 4.0. In assessing the relative range potentialities of possible ram-jet fuels, it was concluded that in spite of its high density, aluminum does not yield so long a range as a hydrocarbon fuel. The most promising fuels investigated for long range were the borohydrides and metallic boron. The range potentialities of the borohydrides and metallic boron were very similar; any choice between them must be based on practical considerations such as cost and ease of application. Aluminum-hydrocarbon slurries were inferior to pure hydrocarbon fuels on a range basis and boron-hydrocarbon slurries were superior to pure hydrocarbons, approaching the practical range potential of pure metallic boron (evaluated at 50 percent of solid-metal density). It was concluded that the practical difficulties associated with the use of liquid hydrogen cannot be justified on a range basis, but if tactical considerations predicate flight at extremely high altitudes, liquid hydrogen must be considered as a possible fuel. The analysis predicted a maximum relative range at an

initial altitude of 70,000 feet and a Mach number of 3.6 when diborane fuel was used. At this flight condition, diborane exhibited a range advantage of 59 percent over the hydrocarbon fuel and an advantage of 5 percent over pentaborane.

INTRODUCTION

The application of ram-jet engines to long-range supersonic aircraft offers unique opportunities for the utilization of specialized fuels. The ability of the ram-jet engine to utilize a wide variety of fuels, and the sensitivity of supersonic aircraft performance to fuel storage requirements make the fuel selection problem for these configurations one of unusual significance.

The range of any aircraft flight depends on the ratio of the propulsive energy obtained from the fuel to the total drag of the airplane. Because the propulsive energy obtained from the fuel is directly proportional to effective heating value (chemical heating value times combustion efficiency), and airplane drag increases with decreasing fuel density, greatest range will result from a fuel having a high effective heating value and a high density. Unfortunately, both of these properties cannot be obtained simultaneously with known chemical fuels, and the manner in which a compromise is made in the selection of a ram-jet fuel becomes of great importance in assessing the range potentialities of the ram-jet airplane.

The nature of this compromise between density and heating value is discussed in reference 1. Inasmuch as the primary object of reference 1 is to study the effects of propulsion system and flight speed on aircraft range, its treatment of the effects of fuel properties was necessarily of a preliminary nature. No attempt was made to adapt the airplane to each particular fuel in order to fully exploit the combination of heating value and density peculiar to that fuel. Even so, important conclusions can be drawn from reference 1 in which it was apparent that fuels other than conventional hydrocarbons must be included in a discussion of ram-jet range potentialities. Furthermore, the suitability of a particular fuel to a specific mission, that is, a particular combination of range, Mach number, and altitude, suggests that it may be desirable to develop several ram-jet fuels.

This report presents the results of an analysis, conducted at the NACA Lewis laboratory, which investigates the effects of fuel heating value and density on ram-jet airplane range in an attempt to broaden understanding of the fundamental advantages or disadvantages of any particular fuel. Any final evaluation of potential ram-jet fuels must be based on cost, availability, logistics, and other practical considerations in addition to range. These practical considerations are beyond

the scope of the present analysis; herein attention is specifically directed toward the range potentialities associated with any combination of fuel density and heating value especially as applied to long-range supersonic missiles. In order to generalize the study as much as possible, fuel heating value and density are treated throughout as independent variables. Actually, range is easily shown to be directly proportional to effective heating value; thus it is convenient to present the results as the dimensionless ratio between aircraft range and fuel effective heating value R/B. The analysis therefore can apply to any fuel by substitution of the values of effective heating value and density applicable to that fuel into the results presented herein.

Throughout the analysis, only design-point performance is considered and every component of the airplane is assumed to be specifically designed for each particular flight condition. In this way, fuel-property effects are isolated as much as possible so that the results may reflect the fundamental relationships between aircraft range and fuel properties. Only cruise is analyzed; take-off and climb are not considered.

The analysis includes fuel densities from 4 to 200 pounds per cubic foot, Mach numbers from 1.5 to 4.0, and initial altitudes from 35,332 to 100,000 feet. Results are presented for an airplane initial gross weight of 150,000 pounds and a pay-load and controls weight of 10,000 pounds.

METHOD

The wide range of conditions included in the analysis made the assumption of flexible airplane and engine designs essential. Therefore, the more important design parameters were not fixed, but were optimized for each condition investigated so that the results would reflect the effects of fuel properties without including the effects of arbitrary design parameters.

The range of conditions investigated also resulted in airplane configurations having very different physical dimensions. The analysis therefore included the effect of Reynolds number on skin friction and allowance was made for the effect of airplane size on structural weight.

Assumptions

A complete list of symbols is given in appendix A. Assumptions describing the aerodynamics of the aircraft components are listed in appendix B, and assumptions describing component weights are presented in appendix C.

All assumptions were made so as to represent long-range missile design. A pay-load and controls weight of 10,000 pounds was assumed and except for a detailed study of the effect of gross weight at a specific flight condition, an initial gross weight of 150,000 pounds was used throughout. Cruising range only was considered, and it was assumed that the aircraft was accelerated to cruising speed and altitude by rocket boost or other external means. Because only one gross weight was considered, the boosting technique at a single altitude and Mach number will apply reasonably well to all fuels, only the physical dimensions of the aircraft being altered by changes in fuel properties. Therefore consideration of boosting would not alter comparisons at a single altitude and Mach number. However, for different Mach numbers and altitudes, different boosting techniques must be assumed and cruising range for fixed aircraft gross weight, although unaffected by boosting considerations, is a less valid criterion for comparisons between these different flight conditions. Booster gross weight, or booster complexity, which is not considered herein, might have a significant effect on the practical advantages of a particular flight condition as compared with other flight conditions.

The cruising range was estimated according to the Breguet range equation for which constant airplane lift-drag ratio and constant thrust-horsepower specific fuel consumption (lbs fuel/thrust hp-hr) throughout the flight are assumed. Theoretically, this flight plan can be nearly realized for the ram-jet airplane by holding flight Mach number and engine temperature ratio constant and causing the altitude to increase as fuel is consumed so that ambient pressure varies directly with gross weight. Except for Reynolds number effects this plan results in constant angle of attack and constant airplane lift-drag ratio throughout cruise and equilibrium flight under these conditions demands that engine thrust vary directly with ambient pressure. Within the limits of the isothermal atmosphere, constant flight Mach number results in constant flight velocity and with constant engine temperature ratio, engine thrust does vary directly with ambient pressure (Reynolds number effects are neglected again). Because ambient temperature is constant in the isothermal atmosphere and a constant engine temperature ratio is assumed, engine temperatures are constant throughout the flight. Except for combustion efficiency and Reynolds number effects, constant fuel-air ratio and constant thrust specific fuel consumption result, and with the constant flight velocity, yield constant thrust horsepower specific fuel consumption as required by the Breguet formula. Outside the isothermal atmosphere, constant flight Mach number results in a flight velocity proportional to the square root of ambient temperature, but constant engine temperature ratio still produces thrust directly proportional to ambient pressure (Reynolds number effects being neglected). This variation of thrust again satisfies the requirements for equilibrium flight at constant angle of attack and constant flight

[redacted]

Mach number, and altitude must increase so that ambient pressure varies directly with gross weight as it does for flight within the isothermal atmosphere. For the case of flight above or below the isothermal atmosphere, constant flight Mach number and constant engine temperature ratio result in an engine fuel-air ratio directly proportional to ambient temperature (except for combustion efficiency and Reynolds number effects and the slight variation in the thermodynamic properties of the working medium with temperature and fuel-air ratio). Therefore the thrust specific fuel consumption of the engine will vary directly with the square root of ambient temperature, and since flight velocity also varies as the square root of ambient temperature, the thrust horsepower specific fuel consumption will remain constant as required by the Breguet formula.

Inasmuch as no particular fuels were considered in analyzing the engine performance, account could not be taken of the effect of combustion-gas properties on the thermodynamic cycle. The products of combustion therefore were assumed to be air. The cycle was calculated with the thermodynamic data of reference 2. No increase in mass flow across the combustor due to fuel addition but simply an addition of heat was recognized. (The effects of these assumptions are demonstrated in RESULTS AND DISCUSSION.) The results of the cycle analysis are expressed as specific heat consumption N' in Btu per second per pound engine thrust minus drag.

A single airplane configuration was assumed, having a triangular plan-form wing and a closed-body fuselage of the Haack class I specifications described in reference 3. The power ducts are mounted externally on the wing, and except for a detailed investigation of the effect of engine size at one flight condition, all engine performance calculations were based on an engine having a combustion-chamber cross-section area of 10 square feet. The various fuel and flight conditions were assumed satisfied by installing various numbers of these units. This assumption avoids the influence of scale effects on engine weight and simplifies the analysis considerably. Furthermore, the engine weight analysis (appendix C) indicated that a combustion-chamber area of 10 square feet would be near the maximum size for minimum specific engine weight for externally mounted engines. Holding engine size constant results in the assumption of a noninteger number of required engines. Actually, a small change in engine size could be assumed so as to reduce or raise the number to an integer. The scale effect associated with such a small change in engine size would not have a significant effect on the results.

No horizontal tail was assumed; the airplane center of gravity was assumed to be fixed during flight and the vertical tail drag was taken as 10 percent of wing zero-lift drag. (These assumptions could also represent a canard or other configuration in which the horizontal tail has the same lift-drag ratio as the wing.) Interference effects between the various aircraft components were approximated by assuming that the

lift and drag of the portions of the wing blanketed by the engines and fuselage were unaffected by the presence of the engines and fuselage. In analyzing each component, only design-point performance was considered and NACA standard atmosphere was assumed.

Optimization of Variables and Determination of Range Parameter

As previously mentioned, the important airplane-design parameters were optimized at each initial cruise condition in order to adapt the airplane as much as possible to each combination of fuel density and flight conditions. Three principal components of the aircraft were considered: wing, engine, and fuselage. At each flight condition and fuel density, it was necessary to make a compromise between weight and efficiency (either aerodynamic or thermodynamic) in arriving at the best component design. This compromise was determined by applying the assumptions of appendixes B and C so as to yield working curves relating weight and efficiency for each of the three airplane components. Wing angle of attack, engine total-temperature ratio, and fuselage-fineness ratio were independently varied in order to obtain these weight-efficiency curves. Partial differentiation of the range equation with respect to each of the three independent variables then revealed the point on the weight-efficiency curve for each component which resulted in greatest aircraft range. Finally, application of the optimum designs thus obtained to the range equation resulted in the final range parameter for each point analyzed. The detailed equations and procedure necessary for the analysis are presented in appendix D.

RESULTS AND DISCUSSION

The principal results of the analysis are summarized in tables I to III and in figure 1. These results are based on an initial gross weight of 150,000 pounds and a pay-load and controls weight of 10,000 pounds and are presented for four initial altitudes; 35,332, 50,000, 70,000, and 100,000 feet. Data for the maximized range analysis from which the essential performance of all the airplane components can be calculated are given in table I. Tables II and III present the characteristics of the wing and engine at conditions for maximum efficiency of each component. The dimensionless range parameter as a function of fuel density for the several Mach numbers and altitudes included in the analysis is plotted in figure 1 from data included in table I.

Effect of Fuel Density

Because the entire fuel load is carried inside the fuselage in the assumed airplane configuration, fuel density effects are produced through the fuselage drag and fuselage structural weight resulting from the particular fuel load. Fuselage drag and fuselage structural weight increase with increasing fuel bulk; therefore a decrease in fuel density always reacts unfavorably on aircraft range as shown in figure 1.

The application of the curves of figure 1 to some specific ram-jet engine fuels of current interest is illustrated in the section entitled "Application of Results to Specific Fuels." However, some general conclusions can be drawn from a study of figure 1 without reference to any specific fuels. The consistent shape of the curves of figure 1 indicates that neither very dense nor very light fuels are likely to be of great importance with regard to range. In general, decreases in fuel density below 30 pounds per cubic foot must be accompanied by very substantial advantages in heating value in order to gain any range advantage. The rapid rise in fuselage weight and fuselage drag accompanying reductions in fuel density below 30 pounds per cubic foot reduces the range potential. For example, as fuel density is decreased from 30 to 4 pounds per cubic foot, fuel bulk per unit weight is increased more than sevenfold. Even after optimizing fuselage-fineness ratio, this decrease in fuel density results in a two- or threefold increase in fuselage drag and fuselage weight. Both of these items react unfavorably on range, reducing the range parameter by 30 to 60 percent. Increases in fuel density above 100 pounds per cubic foot offer little opportunity for increased range. Even an increase in density from 100 to 200 pounds per cubic foot, which is beyond the density of the heaviest fuels now under consideration, results in only a 5 to 20 percent decrease in fuselage weight and fuselage drag. These reductions, in turn, produce an average increase in range of only 7 percent as figure 1 shows. According to existing knowledge of chemical fuels, an increase in fuel density from 100 to 200 pounds per cubic foot will be accompanied by a sharp reduction in fuel effective heating value; thus the limited range advantages of high density fuels are apparent.

A comparison of the various curves of figure 1 indicates that aircraft range is least sensitive to fuel density at high altitudes and low Mach numbers. This insensitivity is apparent in the relatively flat slopes of the curves representing the low Mach number and high-altitude flight conditions, and can be explained by consideration of the effect of altitude and Mach number on the importance of fuselage weight and fuselage drag. The low dynamic pressures associated with low-speed and high-altitude operation require a large wing in order to provide adequate lift. Therefore, wing weight and wing skin area are both large at these flight conditions. Fuselage structural weight is mainly a

function of fuel weight and bulk and is not sensitive to changes in flight conditions. Fuselage drag is directly affected by changes in flight conditions as it is proportional to dynamic pressure and therefore decreases at low Mach numbers and high altitudes. All these factors react on the airplane making wing weight and drag of major importance and fuselage weight and drag of minor importance at low Mach numbers and high altitudes, so that aircraft range is least sensitive to fuel density at these flight conditions.

The curves of figure 1 indicate that considerable attention should be directed toward fuel densities of approximately 35 to 60 pounds per cubic foot because the slope of the curves changes most rapidly at densities just below these values.

Incidental Results

The very rapid deterioration of range with decreasing Mach number below 3.0, which is characteristic of ram-jet airplanes, is demonstrated in figure 1. The effect of altitude is less pronounced, but it is apparent that as altitude is decreased below 50,000 feet or increased above 70,000 feet, range decreases.

The altitudes of table I and figure 1 are the initial cruising altitudes but because of the assumed flight plan, the final cruising altitudes will be somewhat higher, depending on the fuel weight to gross weight ratio. The exact relationship between initial and final cruise ambient pressure and fuel weight to gross weight ratio for a constant Mach number Breguet flight path is

$$\frac{p_{initial}}{p_{final}} = \frac{1}{1 - w_f}$$

For example, for an initial cruising altitude of 70,000 feet and a fuel weight to gross weight ratio of 0.655, the final cruising altitude will be 92,300 feet. Most long-range flights starting at an altitude of 100,000 feet will climb above the upper limit of the isothermal atmosphere (104,987 ft) during cruise. For such flights, constant engine temperature ratio and constant flight Mach number are maintained by varying engine fuel-air ratio directly with ambient temperature and the Breguet range equation is still valid as previously explained.

The optimum wing, engine, and fuselage performance for maximum range listed in table I always occurs at efficiencies lower than the maximum possible for each component. Maximum efficiencies with corresponding component weights are listed for the wing and engine in tables II and III. Minimum fuselage drag and fuselage weight for any

given condition can be calculated from the assumptions described in appendixes B and C. The extent to which the analytical method compromised between weight and efficiency of wing and engine in order to achieve maximum theoretical range is shown by a comparison of tables I, II, and III. Maximum range occurred near maximum component efficiency in all cases; however, important savings in wing and engine weight were realized by deviating slightly from the maximum efficiency conditions. Reductions in wing weight up to 23 percent and reductions in engine weight up to 47 percent were realized by the optimization procedure with corresponding sacrifices up to 10 percent in wing efficiency and up to 15 percent in engine specific heat consumption.

Fuselage-fineness ratio for maximum range was far from the value for minimum fuselage drag in all cases. Fineness ratio for minimum drag per unit volume is approximately 29 for the body shape assumed; whereas optimum fuselage-fineness ratio was less than 16 in all cases as shown in table I. The extremely flat optimum of the fuselage drag against fineness ratio curve for fixed fuselage volume and the steep slope of the fuselage weight against fineness ratio curve combine to produce this result.

Because the engine cycle analysis disregarded the effects of dissociation and fuel addition, the range of optimum engine total-temperature ratios shown in table I is important. At only a few points is operation extended into what might be called the rich fuel-air region. Maximum final gas temperature and maximum combustor heat addition occur at an altitude of 100,000 feet, Mach number of 4.0, and fuel density of 4 pounds per cubic foot, which is near the density of liquid hydrogen. At these conditions, the optimum total-temperature ratio is 3.35, resulting in a combustor outlet temperature of 5520° R. Neglect of dissociation phenomena in this case leads to appreciable error, although the error is not so great as might first be expected. The high flight Mach number involved provides a large available expansion ratio at the combustor exit and the assumption of complete expansion in the exhaust nozzle which was employed throughout the analysis results in relatively low exhaust exit static temperature. If equilibrium conditions are assumed in the expansion process, much of the energy lost by dissociation in the combustor will become available in the exhaust nozzle through the re-association necessary to maintain chemical equilibrium at the lower temperatures. Thus, if equilibrium is maintained in the expansion process, the effects of dissociation are minimized. The effects of exhaust-gas dilution and fuel-weight addition are small for hydrogen in any case. Even at the conditions cited, the fuel-air ratio would be only 0.025 for an effective heating value of 46,400 Btu per pound, which is a representative value for hydrogen. At an altitude of 70,000 feet, Mach number of 3.5, and fuel density of 50 pounds per cubic foot (typical of a hydrocarbon fuel), optimum heat addition requirements are less severe, being satisfied by a total-temperature ratio of 2.32

as shown in table I. Peak cycle temperature would be 3140° R and fuel-air ratio 0.030 for an effective heating value of 16,800 Btu per pound (chemical heating value of 18,650 times combustion efficiency of 90 percent). The effects of dissociation and exhaust-gas composition are negligible in this case.

Fuel weight to initial gross weight ratio listed in column 15 of table I is shown to be quite sensitive to changes in initial cruise altitude. This sensitivity is caused by the necessary increase in wing and engine weight as altitude is increased. The effect is mitigated somewhat by the reduction in fuselage weight accompanying a reduction in fuel weight.

Engine specific heat consumption, shown in column 10 of table I is the heat input in Btu per second divided by the engine thrust minus nacelle drag. Multiplying the specific heat consumption by 3600 over fuel effective heating value in Btu per pound yields the engine specific fuel consumption in pounds per hour per pound of thrust minus nacelle drag. The number of engines required, column 11, is the result of fixing engine size at 10 square feet as explained previously, and is shown to vary between 0.68 and 22.3. This range is obviously outside practical limitations and can only be justified by its simplification of the analytical work. In the most interesting range of flight conditions, that is between 50,000 and 70,000 feet and between Mach numbers of 3.0 and 4.0, the required number of engines was more practical and ranged from 1.24 to 5.87.

Detailed Investigation for Altitude of 70,000 Feet and Mach Number of 3.5

An initial cruising altitude of 70,000 feet and Mach number of 3.5 were selected for an investigation of the effects of several design variables which could not be evaluated in the more general analysis. This detailed investigation served to demonstrate the sensitivity of the final results to changes in some of the principle assumptions. Except where a parameter was deliberately varied over a range of values, assumptions were identical with those used to obtain figure 1. No attempt was made to re-optimize wing angle of attack, engine total-temperature ratio, and fuselage-fineness ratio as each parameter was varied. Instead, the optimum values of these variables at an altitude of 70,000 feet and Mach number of 3.5 as listed in table I were accepted and held constant while the particular design variable being investigated was varied through a range of values. The design variables investigated were diffuser total-pressure ratio, combustion-chamber length-diameter ratio, combustion-chamber area, airplane gross weight, wing angle of attack, engine total-temperature ratio, and fuselage-fineness ratio. Results are presented in figure 2.

The most important conclusions to be drawn from figure 2 are: (1) Comparisons between various fuel densities are not sensitive to changes in the design variables investigated; and (2) the optimum compromises between weight and efficiency as determined by the methods of appendix D for the wing, engine, and fuselage were in good agreement with the true optimums as presented in figures 2(e), (f), and (g).

The effect of diffuser total-pressure ratio on range at the initial altitude of 70,000 feet and Mach number of 3.5 is shown in figure 2(a). Inasmuch as the effect of lip angle on nacelle drag is neglected in the present analysis, figure 2(a) illustrates only the internal effects of diffuser pressure recovery. Inlet geometry suitable for the achievement of very high diffuser total-pressure ratios would probably have to incorporate high lip angles and at these conditions the effect of lip angle on nacelle pressure drag would be appreciable. Even so, the effect of lip angle on range would be negligible because nacelle pressure drag is a small fraction of total airplane drag at the conditions represented in figure 2(a). For example, at a diffuser total-pressure ratio of 0.5 and a fuel density of 50 pounds per cubic foot, nacelle pressure drag (neglecting any effects from lip angle) is 2 percent of total airplane drag. Total-pressure ratios between 0.21 and 1.00 are included in the figure, the higher value corresponds to isentropic recovery and the lower value represents normal shock and a subsonic diffuser recovery of 0.9.

Figure 2(b) demonstrates that combustion-chamber length-diameter ratio has a very minor effect on range. One of the most important effects of combustion-chamber length on engine performance and therefore on range is accomplished through the effect of length on combustion efficiency and combustion pressure losses. Combustion pressure losses were assumed to be independent of combustion-chamber length for this analysis and combustion efficiency is included in the range parameter R/B which is the ordinate of the figure. Therefore the curves of figure 2(b) illustrate only the external effects of combustion-chamber length caused by variations in nacelle drag and engine weight, but their flat slopes are of considerable interest since they demonstrate that little penalty would be incurred if combustion problems necessitated lengthening of the combustion chamber. Figure 2(c) demonstrates only the external effects of engine size on range such as are produced through engine specific weight and neglects the effects of engine size on combustor and diffuser performance. The relative unimportance of engine size as it might affect range through engine specific weight is shown by figure 2(c) and justifies the assumption of a fixed combustion-chamber cross-section area size of 10 square feet which was made in the general analysis. Adjustment of the engine size to some other value in order to obtain a practical number of engines will have little effect on the results as shown by figure 2(c). In constructing the figure, equation (C3) of appendix C was applied without regard to minimum practical

sheet-metal gages for engine fabrication. Appendix C demonstrates that the sheet-metal gages at 10 square feet combustion-chamber area are near the practical minimum. If the sheet-metal gages were assumed to be the minimum allowable at this point, the curves of figure 2(c) would be essentially horizontal to the left of 10 square feet combustion-chamber area. The decrease in range accompanying increased engine size illustrated in figure 2(c) is due to the fact that engine thrust is directly proportional to combustion-chamber area whereas a portion of the engine weight is proportional to combustion-chamber area raised to the 3/2 power. The increase in range accompanying an increase in gross weight with fixed pay-load weight is illustrated in figure 2(d). At the conditions analyzed, the increase in range with increasing gross weight is initially very rapid, but eventually the benefits of increasing size become less pronounced. One reason for this effect can be found in the adverse scale effect included in the wing weight equation. The necessity of supporting the aerodynamic loads farther from the wing root results in less favorable wing weights, which are reflected in the fuel weight that can be carried and ultimately in the range. A further reason for the decreasing benefits of airplane size is the diminishing importance of the fixed pay-load weight as it is applied to ever larger gross weights.

At the conditions analyzed, wing angle of attack and engine total-temperature ratio have a minor effect on range (figs. 2(e) and (f)). The effects would be more pronounced at higher altitudes and lower Mach numbers because of the increased importance of wing and engine performance at these conditions. Figure 2(g) shows that the effect of fuselage-fineness ratio on range is pronounced at an altitude of 70,000 feet and a Mach number of 3.5. For the fuel density of 50 pounds per cubic foot, minimum fuselage drag would occur at a fuselage-fineness ratio of about 29. The optimum fineness ratio for maximum range is near 12 for this fuel density (fig. 2(g)). Extrapolating the data of figure 2(g) shows that range would be reduced approximately 30 percent if the fuselage were designed for minimum drag in this case.

Application of Results to Specific Fuels

The general results presented were applied to six potential ramjet fuels in order to demonstrate some specific comparisons obtainable from the analysis. The six fuels selected were liquid hydrogen, liquid diborane, liquid pentaborane, metallic aluminum, metallic boron, and MIL-F-5624A (JP-3 or JP-4). Two sets of results were obtained for the metallic fuels, one set based on the full solid density of the metal and the other set based on 50 percent of the solid metal density. The 50 percent of solid density condition was included to allow for voids and fuel-handling equipment and is intended to represent a practical figure for present-day solid fuel storage and handling techniques. The full metal density was included to illustrate results for the ultimate

possible achievement in efficient fuel storage and handling techniques. Results for the full metal density are also useful in estimating the performance of metal-liquid fuel slurries.

Some pertinent properties of the six fuels are given in the following table:

Fuel	Phase	Heating value (Btu/lb)	Density (lb/cu ft)	Approximate boiling point (°F)	
				Sea level	70,000 ft
Hydrogen	Liquid	51,604	[a]4.43	[a]-424	[a]-435
Diborane	Liquid	31,080	[a]35.0	[a]-134	[a]-209
Pentaborane	Liquid	29,147	[a]38.1	[a]118	[a]9
Aluminum	Solid	13,318	[a]168.6	-----	-----
Boron	Solid	25,120	[b]144.0	-----	-----
MIL-F-5624A (JP-3 or JP-4)	Liquid	18,652	48.1	106 to 556	[c]-18 to 349

[a]Reference 4.
[b]Reference 5.
[c]Reference 6.

The heating values listed in the table were calculated from the data of reference 7. The fuel was assumed to enter the combustor at 77° F and metal oxides in the products of combustion (if present) were assumed to be solids. No heat was diverted to heat the mass of the fuel itself (or an equivalent mass of products) to combustor outlet conditions. This latter assumption was included to be consistent with the assumption of zero mass-flow increase across the combustor which was mentioned previously in the discussion of the cycle calculations. One important property pertinent to any comparison of various fuels is the efficiency with which the fuels can be burned in a practical combustion chamber at the flight conditions under consideration. No attempt was made herein to consider this fuel property; the comparison between the six ram-jet fuels was based on equal combustion efficiency for all fuels. Achieving satisfactory combustion efficiency at the high altitude and low Mach number flight conditions would probably be difficult with some of the fuels considered. Even so, a comparison of the various fuels on the assumption of equal combustion efficiencies is valuable as an index of the fundamental range relations associated with fuel density and heating value. Any refinement of these relations so as to include combustion efficiency effects can be easily accomplished inasmuch as aircraft range is directly proportional to combustion efficiency.

Although selection of the six fuels from the many which might be considered for ram-jet application was somewhat arbitrary, the following reasoning was applied: Hydrogen was considered because it offers a unique combination of heating value and density; the borohydrides were chosen over other hydrides because of their outstanding range potential; boron was included because of its great range potential as compared with other solid fuels. Beryllium might merit equal consideration with boron but its toxicity makes it less desirable. Aluminum was taken as typical of fuels such as aluminum, magnesium, and carbon; MIL-F-5624A (JP-3 or JP-4) was chosen as a typical hydrocarbon fuel.

Results obtained for the six fuels are presented in figure 3 as range relative to the range of MIL-F-5624A (JP-3 or JP-4) at 70,000 feet and a Mach number of 3.5. On the basis of range, the most promising fuels investigated were the borohydrides (diborane and pentaborane) and metallic boron. The range potentialities of these three fuels were very similar; any choice between the three would have to be based on practical considerations such as cost and ease of application.

The full-density and half-density curves of each of the metallic fuels provide a convenient means of observing the effect of improvements in solid fuel storage and handling techniques. At no point does the full-density curve for a particular solid fuel surpass the half-density curve by more than 15 percent and at the more practical flight conditions the improvement is less than 8 percent. Inasmuch as considerable refinement in technique is necessary even to achieve performance halfway between the full-density and half-density curves, little or no improvement is to be expected from this source. This premise is a direct result of the conclusion derived from figure 1, that range is not sensitive to improvements in fuel density above densities of approximately 100 pounds per cubic foot.

In spite of its high density, aluminum did not yield as great a range as the hydrocarbon fuel under any condition investigated (fig. 3). Even the full-density aluminum curve is inferior to MIL-F-5624A (JP-3 or JP-4) at all points. The performance of aluminum slurries in a hydrocarbon base can be approximated by interpolating between the curves representing MIL-F-5624A (JP-3 or JP-4) and full-density aluminum. The range performance for such slurries will fall short of the range for the hydrocarbon fuel at all conditions because of the decreased heating value available from such slurries and the relative unimportance of the increased density which they provide. The inferior performance of aluminum and magnesium fuels is limited to long-range operation. For short-range ram-jet engine applications, especially those requiring high thrust output, the aluminum and magnesium fuels may be superior.

Boron-hydrocarbon slurries offer increased range as shown by interpolation between the MIL-F-5624A (JP-3 or JP-4) fuel and full-density

boron curves of figure 3. At 70,000 feet and Mach number of 3.5, an 80 percent boron slurry would result in a relative range approximately as great as the pure boron fuel, provided the pure boron is evaluated at a density equal to half the solid metal density. Successful application of an 80 percent boron slurry is somewhat beyond present-day techniques; however, the comparison is of value in pointing out possible advantages which may be derived from boron slurries.

The successful application of liquid hydrogen presents tremendous practical difficulties arising from the extremely low temperature, high pressure, or both necessary to maintain it as a liquid. In constructing figure 3, no extra penalties were applied to liquid hydrogen in order to allow for the weight and bulk of equipment necessary to guarantee safe storage of the fuel during the flight. Therefore the results presented in figure 3 are the most optimistic possible with regard to liquid hydrogen and the difficulties inherent in its use cannot be justified on the basis of range. However, it is important to note that at very high altitudes hydrogen is markedly superior to the other fuels and its range potential is only 15 percent less than the best range predicted for any other fuel at lower Mach number and altitude. If tactical considerations predicate flight at extremely high altitudes, liquid hydrogen must be considered as a possible fuel.

Maximum relative range predicted in figure 3 was 1.59 for diborane at an initial cruise altitude of 70,000 feet and Mach number of 3.6. The results show a relative range of 1.51 for pentaborane at these conditions.

CONCLUDING REMARKS

An analysis was presented of the effect of fuel density and heating value on the cruising range of a ram-jet airplane suitable for application to long-range supersonic missiles. The analysis was based on an airplane initial gross weight of 150,000 pounds and a pay-load and controls weight of 10,000 pounds. Only a solid body fuselage and externally mounted engines were considered. The following conclusions were drawn from the analysis:

1. Use of fuel densities lower than 30 pounds per cubic foot will probably reduce aircraft range because of the very rapid deterioration of range with decreasing density below this value. Also, fuel densities larger than 100 pounds per cubic foot are not desirable because of the slow increase in range with increasing densities above this value. Fuel densities in the range of 35 to 60 pounds per cubic foot appear best for long range missions.

[redacted]

2. For a given heating value, aircraft range is most sensitive to changes in fuel density at low altitudes and high Mach numbers.

3. The fuels investigated which appear to offer greatest advantages of range are the borohydrides (diborane and pentaborane) and metallic boron. The range potentialities of these three fuels were shown to be very similar; any choice between the three would have to be based on practical considerations such as cost and ease of application.

4. The range potentialities of boron-hydrocarbon slurries are considerably above the potentialities of pure hydrocarbon and may approach the practical range potential of metallic boron (evaluated at 50 percent of solid metal density).

5. In spite of its high density, aluminum did not yield as great range as the hydrocarbon fuel and the range potentialities of aluminum slurries in a hydrocarbon base are inferior to pure hydrocarbon at all conditions investigated.

6. The practical difficulties associated with the use of liquid hydrogen cannot be justified on a range basis, but if tactical considerations predicate flight at extremely high altitude, liquid hydrogen must be considered as a possible fuel.

7. Maximum range predicted by the analysis occurred at an initial cruising altitude of 70,000 feet and a Mach number of 3.6. At these conditions, the range of diborane relative to the hydrocarbon fuel was 1.59 and the relative range of pentaborane was 1.51.

Lewis Flight Propulsion Laboratory
National Advisory Committee for Aeronautics
Cleveland, Ohio

[redacted]

APPENDIX A

SYMBOLS

The following symbols are used in this report:

A	frontal area, sq ft
A_c	combustion-chamber area, sq ft
a	speed of sound, ft/sec
B	fuel heating value times combustion efficiency
C_F	skin friction drag coefficient based on wetted area
C_T	wave drag coefficient based on frontal area
D	drag of aircraft component divided by aircraft gross weight
d	diameter
F	net thrust minus drag of all engines divided by aircraft gross weight
f	fineness ratio
J	mechanical equivalent of heat, 778 ft-lb/Btu
K	constant
M	Mach number
N'	engine specific heat consumption, Btu/sec/lb thrust minus drag
p	static pressure, lb/sq ft
q	incompressible dynamic head, $\frac{\gamma}{2} pM^2$, lb/sq ft
R	aircraft range
Re	Reynolds number
S	wing area, sq ft
s	wetted area, sq ft
U	engine specific weight, lb engine/lb thrust minus drag

[redacted]

V	volume, cu ft
W	aircraft initial gross weight, lb
w	weight of aircraft component divided by aircraft initial gross weight
x,y	coordinate system for definition of fuselage shape and nacelle shell shape
α	wing angle of attack, radians
γ	ratio of specific heats for air
λ	length
τ	engine total temperature ratio
ρ	density, lb/cu ft

Subscripts:

0	ambient free-stream conditions
d	diffuser
e	engine
ei	engine inner shell
f	fuel
H	class I Haack body
n	nacelle
p	pay-load and controls
s	fuselage
t	ogive
w	wing and tail

APPENDIX B

COMPONENT AERODYNAMICS

To facilitate the analysis, the aircraft was divided into three principle components and the aerodynamics of each component were analyzed separately. Consistent (as possible) assumptions were applied. The design-point performance of the complete aircraft was then assumed equal to the sum of the design-point performances of its component parts.

In general, aerodynamic forces were obtained from the literature based on three-dimensional linearized theory originally developed in reference 8.

External skin friction drag was calculated according to the following equation:

$$C_F = \frac{0.0306\ K}{Re^{1/7}\left[1 + \frac{\gamma-1}{4} M_O^2\right]^{5/7}} \qquad (B1)$$

Equation (B1) was obtained by use of the flat-plate formula of reference 9 in which the temperature of the boundary-layer air is assumed to be the arithmetic mean of wall and free-stream temperature. Reynolds number in equation (B1) is based on free-stream conditions. In applying the flat-plate formula of reference 9, the K appearing in equation (B1) was added to account for the effect of body geometry on skin-drag coefficient. In the present analysis, K was taken as 1.03 for the wing and 1.05 for the nacelle and fuselage.

Wing and Tail

In order to include the tail calculations with the wing calculations, it was assumed that tail performance was a direct function of wing performance. No horizontal tail was assumed; the airplane center of gravity was assumed to be fixed during flight, and vertical tail drag was assumed equal to 10 percent of wing zero-lift drag.

Geometry. - For maximum flexibility, variable wing geometry could be assumed and securing the most advantageous wing at each condition could be accomplished by adjusting wing weight and wing efficiency through wing geometry. No attempt was made to do this in the present analysis but somewhat the same effect was achieved in a simpler manner by keeping wing geometry fixed and adjusting wing weight and wing efficiency through angle

of attack so as to achieve maximum range. The following fixed wing geometry was assumed:

Plan form	triangular
Section	biconvex
Thickness ratio, percent	$3\frac{1}{2}$
Aspect ratio	3
Maximum thickness point, percent of chord	50

2334

Lift and drag. - The pressure drag of a biconvex airfoil at supersonic velocities is not easily obtained by three-dimensional linearized theory. Therefore, it was assumed that the pressure drag of the $3\frac{1}{2}$-percent thick biconvex section was equal to 1.3 times the pressure drag of a $3\frac{1}{2}$-percent thick double-wedge section.

Pressure drags for the double-wedge section were obtained from reference 10.

The pressure drags of wings of the type used herein, calculated by a rational but lengthy method are presented in reference 11, which was published after completion of the present analysis. A comparison of the pressure drags calculated in the present analysis with the data of reference 11 reveals differences of less than 6 percent in all cases.

Skin friction drag was calculated by use of equation (B1) with K equal to 1.03 and Reynolds number based on the mean geometric chord.

Wing lift was obtained from reference 12. No leading-edge suction was assumed.

Engine External Flow

Geometry. - The geometry of the power ducts is shown in figure 4. This geometry was assumed throughout the analysis except for the detailed study at one flight condition of the effects of combustion chamber length-diameter ratio.

As shown in figure 4, an over-all engine length of 9 combustion-chamber diameters was assumed. The diffuser section was 4, the combustion chamber 3, and the nozzle section 2 diameters long. The entire engine duct was surrounded by a nacelle shell. For the boattailed nacelle (necessary at low flight Mach number and small heat addition), a nacelle

shell diameter 1.2 times the combustion-chamber diameter was assumed. The nacelle shell was assumed to be composed of two open-nosed tangent ogives of equal length, each consisting of a segment of a Haack class I body. This body, originally proposed by Haack (reference 13), develops minimum pressure drag for a given enclosed volume and a given fineness ratio. The equation of the silhouette of such a body, derived from reference 3, is:

$$y = \left(\frac{d_n}{2}\right)\left[1 - \left(\frac{2x}{\lambda_H}\right)^2\right]^{3/4} \qquad (B2)$$

As flight Mach number or engine heat addition is increased, less boattailing is necessary and when the engine outlet diameter reaches 1.2 times combustion-chamber diameter, the nacelle downstream ogive becomes a cylinder and the shell may be described as a flared nacelle. For still larger outlet diameters, the length of the cylindrical section is reduced so that the diameter of the nacelle upstream ogive at the midpoint of the nacelle is always at least 1.2 times the combustion-chamber diameter.

For highly flared nacelles (necessary at high flight Mach numbers and large heat addition), the length of the cylindrical section diminishes to zero so that the nacelle shell consists of a single open-nosed tangent ogive consisting of a segment of the body defined by equation (B2).

Drag. - The nacelle pressure drag was calculated by considering each tangent ogive separately. It was assumed that the pressure drag of any of the open-nosed ogives was equal to one-half the pressure drag of the Haack body of which it was a segment multiplied by 1 minus the ratio of ogive minimum area to ogive maximum area. This assumption implies that pressure drag is proportional to net frontal area and ogive pressure drag is the same, regardless of whether the ogive is pointed upstream or downstream. These assumptions are similar to those employed in references 1 and 14. Recent experimental results indicate that this method of estimating nacelle pressure drag may lead to appreciable errors, especially for boattailed nacelles. However, the method is simple and readily applied and nacelle drag is a small fraction of total airplane drag in most cases. For instance, the analytical results showed that at an altitude of 70,000 feet and a Mach number of 3.5 and for a fuel density of 50 pounds per cubic foot the nacelle pressure drag is only 2.0 percent of total airplane drag; aircraft range would be extremely insensitive to changes in nacelle pressure drag in this case. The optimum engine temperature ratio for maximum range, which depends on the relation between engine weight and engine thrust minus drag, would be somewhat more sensitive to changes in nacelle pressure drag.

The pressure drag coefficient of a complete closed body of the assumed shape, from reference 3 is:

$$C_T = \frac{9\pi^2}{8f_H^2} \qquad (B3)$$

It was assumed that this equation described the pressure drag at a flight Mach number of 1.5. At higher flight Mach numbers, the pressure drag coefficient was empirically decreased by applying the data of reference 15 as suggested in reference 1. The cone pressure drag data of reference 15 was plotted against cone angle and flight Mach number. The variation of pressure drag with Mach number was then obtained by defining an equivalent cone as that cone whose pressure drag at Mach number 1.5 according to reference 15 was equal to one-half the pressure drag described by equation (B3). It was then assumed that the pressure drag of the body under consideration varied with Mach number in exactly the same manner as described in reference 15 for the equivalent cone just described.

Because the analysis was confined to design-point conditions, no additive drag or base drag was assumed for the nacelle. The effect of lip angle on nacelle pressure drag was neglected because the assumed schedule of diffuser pressure ratios could probably be realized by low-lip-angle inlet geometries and because the assumed nacelle shell ogive could tolerate some lip angle without altering external nacelle geometry.

Nacelle skin friction drag was calculated according to equation (B1) with K equal to 1.05 and Reynolds number based on the nacelle length. Except for the detailed study at the specific flight condition of the effect of engine size, a single engine size of combustion-chamber cross-section area of 10 square feet was assumed throughout the analysis.

The skin area of an open-nosed tangent ogive of the type defined by equation (B2) can be obtained by integration of a simple binomial expansion. The result is:

$$s_t = \pi d_n \lambda_t \left[1 + \frac{(-3/4)}{(1)}\left(\frac{1}{3}\right)\left(\frac{2\lambda_t}{\lambda_H}\right)^2 + \frac{(-3/4)(1/4)}{(1)(2)}\left(\frac{1}{5}\right)\left(\frac{2\lambda_t}{\lambda_H}\right)^4 + \frac{(-3/4)(1/4)(1\frac{1}{4})}{(1)(2)(3)}\left(\frac{1}{7}\right)\left(\frac{2\lambda_t}{\lambda_H}\right)^6 + \cdots\right] \qquad (B4)$$

[redacted]

Engine Internal Flow

The engine thrust was calculated by use of one-dimensional flow theory. The working medium was assumed to be air throughout the cycle and thermodynamic data were obtained from reference 2, which includes the effects of temperature on the properties of air of fixed composition, but does not include the effects of dissociation. An inconsequential error is introduced in the cases in which the aircraft climbs above the upper limit of the isothermal atmosphere, because the engine cycle was calculated on the assumption that ambient temperature was equal to the temperature of the isothermal atmosphere. Above the isothermal atmosphere, ambient temperatures would be slightly higher so that the thermodynamic properties of air obtained from reference 2 would be in error inasmuch as these properties change slightly with temperature.

Diffuser. - A spike-type multiple-shock diffuser was assumed. Except for the investigation of the effect of diffuser recovery at one flight condition, a single schedule of diffuser performance was used throughout the analysis. Diffuser total-pressure ratios at the various Mach numbers are tabulated as follows:

Mach number M_0	Diffuser total-pressure ratio
1.5	0.950
2.0	.930
2.5	.815
3.0	.670
3.5	.500
4.0	.315

Diffuser-outlet Mach number was taken as 0.2 for all flight Mach numbers where a combustion chamber area larger than diffuser capture area would result. Using the assumed schedule of diffuser recoveries resulted in a diffuser-outlet Mach number of 0.2 at all flight Mach numbers below 3.08. At higher flight Mach numbers, the diffuser-outlet Mach number was adjusted so that diffuser outlet area was exactly equal to diffuser capture area. Using the assumed schedule of diffuser recoveries resulted in diffuser-outlet Mach numbers of 0.1736 and 0.1746 for flight Mach numbers of 3.5 and 4.0, respectively.

To check the validity of the ratio of diffuser length to outlet diameter of 4 assumed throughout the analysis, the equivalent included conical expansion angle of the subsonic internal-flow passage was calculated for all Mach numbers. For typical inlets capable of achieving

the assumed recoveries, the equivalent included conical expansion angle of the internal flow passage was between 5.6° and 6.1° in all cases, which justifies the assumed diffuser fineness ratio.

Combustion chamber. - The combustion-chamber inlet Mach number was assumed equal to diffuser-outlet Mach number. A constant-area burner was assumed and total-pressure loss due to friction was assumed equal to twice the burner inlet incompressible dynamic pressure. Burner momentum pressure loss was obtained from reference 16 on the assumption that all friction losses preceded the heat addition.

Nozzle. - Complete expansion to atmospheric pressure through a convergent-divergent nozzle was assumed in all cases. The polytropic efficiency of the exhaust nozzle was taken as 95 percent, where polytropic efficiency is defined as $\left(\frac{\gamma}{\gamma-1}\right)\frac{\text{log of nozzle temperature ratio}}{\text{log of nozzle pressure ratio}}$

Fuselage

Geometry. - The fuselage was a closed Haack body described by equation (B2). A volume of 450 cubic feet was allowed inside the fuselage for pay load, controls, and unusable space. The remaining fuselage volume was assumed to be entirely filled with fuel. The maximum cross-sectional area of the fuselage A_s was obtained using the following equation, derived from reference 3:

$$A_s = \frac{4(V_s)^{2/3}}{(9\pi)^{1/3}(f_s)^{2/3}} \qquad \text{(B5)}$$

The fuselage skin area s_s can be obtained from equation (B4) by considering the fuselage made up of two identical closed tangent ogives. The result is:

$$s_s = 2.878\ f_s A_s \qquad \text{(B6)}$$

Drag. - The fuselage pressure drag was calculated from equation (B3) at a flight Mach number of 1.5 and correction for the effect of Mach number was made as described previously. Skin friction drag was obtained from equation (B1) for a value of K of 1.05 and a Reynolds number based on fuselage length. Fuselage angle of attack was assumed to be zero, resulting in zero fuselage lift.

APPENDIX C

COMPONENT WEIGHTS

The analysis calls for expressions describing the variation of each component weight with size, geometry, and loading. Accurate determination of these expressions could only result from a detailed design study and even then the expressions would depend to some extent on the ingenuity of the designer. Such a study is beyond the scope of this analysis. Furthermore, accuracy of this order is not required herein because the main purpose of the weight expressions is to effect a compromise with the aerodynamic assumptions so as to achieve balanced results.

For example, figure 5 shows wing drag-lift ratio plotted against wing weight for one flight condition. The wing weight values are approximate, because they are not based on actual design data. If the drag-lift ratio values are correct, some errors in wing weight could be partly compensated for by aerodynamic considerations. If the weights assumed were all too low and the correct curves lie to the right of those illustrated, applying these correct curves to the optimization portion of the analysis would result in a higher optimum angle of attack than would be found for the present curves and would result in a somewhat larger drag-lift ratio. Thus the optimization would mitigate the effects of the change in wing weight by reducing the wing lift-drag ratio somewhat. The advantage of this procedure lies in the fact that errors in the weight assumptions are absorbed to some extent in the aerodynamic analysis, so that their effects on the final results are not as drastic as they would be if fixed angle of attack were assumed. For the present analysis, the weight assumptions can be rather general in nature without greatly affecting the significance of the results.

The form of each weight expression was derived by elementary dimensional considerations. The constants in the expression were then evaluated by applying the equation to a particular component configuration whose weight was known or assumed. Materials and design were assumed adequate so that the structures could function in the assumed environment up to flight Mach numbers of 4.0 without loss of strength due to aerodynamic heating; therefore, no temperature corrections were included in the weight equations.

Wing and Tail

Conventional semimonocoque construction was assumed for wing and tail and the weight was divided into two categories; skin and skin stiffening weight, and weight of material necessary to resist bending.

This elementary weight breakdown is for analytical purposes only, and does not imply that in practice the skin cannot resist bending or that the spars cannot help stiffen the skin. Therefore, the assumption of an effective skin thickness does not imply that the skin must be this same thickness at all points, but is meant to account for that part of the wing weight which is necessary to provide a stiff wing covering capable of transmitting the aerodynamic loads to the bending and shear members. Elastic characteristics were not analyzed, but the weights and geometry are conservative enough so that stiff wings should be possible in all cases. All material was assumed to be stainless steel having a density of 490 pounds per cubic foot. No horizontal tail was included and if vertical tail area is assumed proportional to wing area, the weight of the vertical tail can be included in the wing skin weight term.

Minimum allowable effective skin gage was taken as 0.015 inch for a wing loading of zero and was assumed to be a linear function of wing loading increasing to 0.065 inch at a wing loading of 150 pounds per square foot. This skin weight was assumed to include all necessary skin stiffening members. For fixed wing geometry, dimensional analysis demonstrates that the weight necessary to resist bending is proportional to the square root of wing area. Adding skin and bending weights together gives:

$$w_w = \frac{1.22}{(W/S)} + 0.0271 + K\sqrt{S} \qquad (C1)$$

To evaluate K, the following specific wing was assumed and substituted into equation (C1):

Gross weight, W, lb	100,000
Wing loading, W/S, lb/sq ft	150
Aspect ratio	3.0
Thickness ratio, percent	$3\frac{1}{2}$
Normal load factor	2.0
Wing weight, w_wW, lb	8,810

The final wing weight equation is then:

$$w_w = \frac{1.22}{(W/S)} + 0.0271 + 0.002048\sqrt{S} \qquad (C2)$$

The results of the wing analysis are typified by figure 5, which illustrates wing performance at an altitude of 70,000 feet and Mach

number of 3.5 for an initial gross weight of 150,000 pounds. Wing performance at angle of attack for minimum wing drag-lift ratio is listed in table II.

Engine

Engine weight was considered in three parts: (1) diffuser and associated weight, (2) combustion chamber and nozzle, and (3) outer shell. The entire engine was assumed to consist of stainless steel having a density of 490 pounds per cubic foot.

The inner shell (parts (1) and (2)) was designed to withstand an internal pressure of 93.4 pounds per square inch gage. This pressure is equivalent to a flight Mach number of 2.0 at sea level (for a diffuser total-pressure ratio of 0.94) or a flight Mach number of 3.0 at 30,000 feet (for a diffuser total-pressure ratio of 0.67). The former condition might represent a homing dive under power and the latter is a typical climbing condition. In either case, the hoop stresses in the inner shell would be more severe for these conditions than for most cruise operations; therefore the inner shell was designed for 93.4 pounds per square inch gage, internal pressure. The nacelle outer shell thickness was taken as independent of size or pressure and constant wall thickness along the length of each engine component was assumed.

The assumptions necessary to develop the weight equation are summarized below:

Internal pressure, lb/sq in. gage	93.4
Diffuser allowable stress, lb/sq in.	100,000
Diffuser island, frame and flame holder weight, percent of diffuser shell weight	200
Combustor and nozzle allowable stress, lb/sq in.	50,000
Nacelle outer shell effective gage, in.	0.020

Although the allowable stresses for the diffuser and combustor may have to be reduced for operation at high Mach numbers and associated high stagnation temperatures, the altitude for most cruise operation at these high Mach numbers would be sufficiently high so that internal pressure would be much less than the design pressure of 93.4 pounds per square inch.

Application of these assumptions to the engine geometry illustrated in figure 4 results in the final engine-weight equation:

$$\text{engine weight} = 490 \left[0.002802\ s_d \sqrt{A_c/\pi} + 0.001868\ (s_{ei}-s_d)\sqrt{A_c/\pi} + 0.00167\ s_n\right] \qquad (C3)$$

Application of the assumptions listed previously to an engine size of combustion-chamber area of 10 square feet will result in a diffuser skin thickness of 0.020 inch, and a combustion-chamber and nozzle thickness of 0.040 inch. Each of these gages is probably near the practical minimum. Decreasing engine size below 10 square feet combustion-chamber area therefore yields no decrease in engine specific weight because both engine weight and thrust decrease directly with combustion-chamber area for the fixed engine geometry illustrated in figure 4. Increasing engine size above 10 square feet combustion-chamber area will result in larger specific weights because thrust increases directly with combustion-chamber area whereas a portion of the engine weight increases with combustion-chamber area raised to the 3/2 power. Therefore, an engine size of 10 square feet combustion-chamber area appears to be near the largest size possible for minimum specific engine weight and for this reason, this engine size was assumed throughout the analysis.

The results of the engine analysis are typified by figure 6, which illustrates engine performance at an altitude of 70,000 feet and Mach number of 3.5. Engine characteristics at the total-temperature ratio for minimum speicific heat consumption are listed in table III.

Fuselage

For consistency, fuselage weight assumptions were patterned after wing weight assumptions wherever possible. Conventional semimonocoque construction was assumed, and the fuselage structural weight was broken down into three categories: (1) skin and skin stiffening weight, (2) fuel cell weight, and (3) weight of material necessary to resist normal bending loads. As in the wing weight analysis, this arbitrary weight breakdown does not imply that in practice each structural component would serve only the function assigned to it. The breakdown is assumed so that variations in fuselage structural weight with fuselage geometry and fuselage loading can be included in the analysis. Fuselage material was assumed to be stainless steel having a density of 490 pounds per cubic foot.

A rigid fuselage is desirable, especially for the boosting phase of the flight. If the fuselage is subjected to a 5G gross axial acceleration during boost, hoop stresses are introduced in the fuselage shell because of the pressure of the full fuel load being accelerated within the fuselage. The fuselage skin structure might be effective in withstanding at least part of these hoop stresses as well as the column forces due to the axial acceleration. A 1/16-inch equivalent fuselage skin gage should be adequate in most cases and this gage was assumed through the analysis, thus

$$\text{fuselage skin and skin stiffening weight} = 2.552\ s_s \qquad (C4)$$

Because the fuselage is assumed to be almost entirely filled with fuel, fuel cell weight was considered to vary directly with fuselage skin area. Also, because the fuel cells must seal against the high pressures induced in the fuel as a result of the axial acceleration experienced during boost, the fuel cell weight was made proportional to this induced pressure. If the fuselage is considered as a single fuel tank, the pressure at the bottom of the tank during axial acceleration is proportional to fuselage length times fuel density. Thus

$$\begin{aligned} &\text{fuel cell weight} \propto \text{fuselage length } (\rho_f s_s) \\ &\text{fuel cell weight} \propto f_s w_f W \end{aligned} \qquad (C5)$$

The weight of the stringers necessary to resist bending forces from simple dimensional analysis is:

$$\text{stringer weight} \propto w_f W (f_s)^{3/2} (s_s)^{1/2} \qquad (C6)$$

Total fuselage weight was expressed by adding skin, fuel cell, and stringer weights together and evaluating the constants for a particular condition. The fuselage for which the constants were evaluated was assumed to have the following characteristics:

Fuel weight, $w_f W$, lb	60,000
Fuselage fineness ratio, f_s	12
Fuel density, ρ_f, lb/cu ft	45
Volume, V_s, cu ft	$\frac{60,000}{45} + 450$
Fuel cell weight, lb	6000
Normal load factor	2.0
Axial load factor	5.0
Structural weight, $w_s W$, lb	12,000

The resulting fuselage weight equation is:

$$w_s = \frac{2.552\ s_s}{W} + w_f \left[0.008333\ f_s + 0.03067\ (10)^{-3}(f_s)^{3/2}(s_s)^{1/2}\right] \qquad (C7)$$

The result of the fuselage calculations are typified by figure 7, which illustrates the fuselage performance at 70,000 feet altitude and Mach number 3.5 for a fuel density of 50 pounds per cubic foot, and a fuel weight to gross weight ratio of 0.65.

2334

[redacted]

APPENDIX D

OPTIMIZATION

At each flight condition and fuel density investigated, the wing angle of attack, engine total-temperature ratio, and fuselage fineness ratio were optimized with respect to range.

Derivation of equations. - The airplane is assumed to be in equilibrium flight with the engines operating at their design point. Thus

$$\begin{aligned} D_w + D_s &= F \\ U(D_w + D_s) &= w_e \end{aligned} \tag{D1}$$

The gross weight is assumed to be made up only of fuel weight, fuselage structure weight, engine weight, wing weight, and pay-load and controls weight. No horizontal tail was assumed and the weight of the vertical tail is included in wing weight. Thus

$$1 = w_f + w_s + U(D_w + D_s) + w_w + w_p \tag{D2}$$

If the Breguet range equation is used, the dimensionless ratio R/B can be expressed:

$$\frac{R}{B} = \frac{M_0 a_0}{JN'(D_w+D_s)} \log_e \left(\frac{1}{1-w_f}\right) \tag{D3}$$

Combining (D2) and (D3) gives

$$\frac{R}{B} = \frac{M_0 a_0}{JN'(D_w+D_s)} \log_e \left[\frac{1}{w_s + U(D_w+D_s) + w_w + w_p}\right] \tag{D4}$$

In order to maximize R/B with respect to the three independent variables α, τ, and f_s, three simultaneous equations must be satisfied to establish necessary conditions:

$$\frac{\partial(R/B)}{\partial\alpha} = 0 \tag{D5}$$

$$\frac{\partial(R/B)}{\partial\tau} = 0 \tag{D6}$$

$$\frac{\partial(R/B)}{\partial f_s} = 0 \tag{D7}$$

Sufficient conditions are assumed to be adequately demonstrated by the curves of figures 5 to 7, which are typical of those used in the optimization procedure. Sufficiency is further demonstrated by figures 2(e) to (g). Equation (D4) is used and equation (D5) becomes:

$$\frac{\partial(R/B)}{\partial\alpha} = 0 = -\frac{\left[w_s+U(D_w+D_s)+w_w+w_p\right]\left(U\frac{dD_w}{d\alpha}+\frac{dw_w}{d\alpha}\right)}{(D_w+D_s)\left[w_s+U(D_w+D_s)+w_w+w_p\right]^2} -$$

$$\frac{1}{(D_w+D_s)^2}\log_e\left[\frac{1}{w_s+U(D_w+D_s)+w_w+w_p}\right]\frac{dD_w}{d\alpha}$$

Total derivatives are permissible on the right side of the equation because D_w and w_w are not functions of τ or f_s. Dividing by $\frac{dw_w}{d\alpha}$ and simplifying give:

$$\frac{dD_w}{dw_w} = \frac{-1}{\frac{\left[w_s+U(D_w+D_s)+w_w+w_p\right]}{(D_w+D_s)}\log_e\left[\frac{1}{w_s+U(D_w+D_s)+w_w+w_p}\right]+U} \tag{D8}$$

Equation (D4) is used to give equation (D6) in the form:

$$\frac{\partial(R/B)}{\partial\tau} = 0 =$$

$$\frac{-1}{N'}\frac{\left[w_s+U(D_w+D_s)+w_w+w_p\right]}{\left[w_s+U(D_w+D_s)+w_w+w_p\right]^2}(D_w+D_s)\frac{dU}{d\tau} -$$

$$\frac{1}{N'^2}\log_e\left[\frac{1}{w_s+U(D_w+D_s)+w_w+w_p}\right]\frac{dN'}{d\tau}$$

Total derivatives are permissible on the right side of the equation because U and N' are not functions of α or f_s. Dividing by $\frac{dU}{d\tau}$ and simplifying and substituting for $\frac{dN'}{N'}$ its equivalent, $d(\log_e N')$ yield

$$\frac{d(\log_e N')}{dU} = \frac{-1}{\frac{\left[w_s+U(D_w+D_s)+w_w+w_p\right]}{D_w+D_s} \log_e \left[\frac{1}{w_s+U(D_w+D_s)+w_w+w_p}\right]} \qquad (D9)$$

Through the use of equation (D4), equation (D7) becomes:

$$\frac{\partial(R/B)}{\partial f_s} = 0 = \frac{-\left[w_s+U(D_w+D_s)+w_w+w_p\right]\left(U\frac{dD_s}{df_s}+\frac{dw_s}{df_s}\right)}{(D_w+D_s)\left[w_s+U(D_w+D_s)+w_w+w_p\right]^2}$$

$$-\frac{1}{(D_w+D_s)^2}\log_e\left[\frac{1}{w_s+U(D_w+D_s)+w_w+w_p}\right]\frac{dD_s}{df_s}$$

Total derivatives are permissible on the right side of the equation because D_s and w_s are not functions of α or τ. Dividing by $\frac{dw_s}{df_s}$ and simplifying give

$$\frac{dD_s}{dw_s} = \frac{-1}{\frac{\left[w_s+U(D_w+D_s)+w_w+w_p\right]}{D_w+D_s}\log_e\left[\frac{1}{w_s+U(D_w+D_s)+w_w+w_p}\right]+U}$$

Multiplying by $10^3/q_0$ to obtain a more convenient form gives

$$\frac{d\left(D_s\frac{10^3}{q_0}\right)}{dw_s} = \frac{-\frac{10^3}{q_0}}{\frac{\left[w_s+U(D_w+D_s)+w_w+w_p\right]}{D_w+D_s}\log_e\left[\frac{1}{w_s+U(D_w+D_s)+w_w+w_p}\right]+U} \qquad (D10)$$

Combining equations (D8), (D9), and (D10) results in

$$\frac{dD_w}{dw_w} = \frac{1}{\frac{dU}{d(\log_e N')} - U} = \frac{q_0}{10^3} \frac{d\left(D_s \frac{10^3}{q_0}\right)}{dw_s} \qquad \text{(D11)}$$

In order to apply equations (D8), (D9), and (D10), the relations between weight and efficiency for the wing, engine, and fuselage must be described. The methods used to obtain these relations are outlined in appendixes B and C and the results are typified by figures 5 to 7. For this phase of the calculation, the fuselage data, such as that shown in figure 7, were calculated for a constant value of skin friction drag coefficient $C_{F,s}$ of 0.0015. Therefore, the optimization phase of the analysis disregarded the effect of Reynolds number on fuselage skin drag. The effect of Mach number on nacelle and fuselage pressure drag was also disregarded for this phase and equation (B3) was used to describe the pressure drag of nacelle and fuselage bodies for all Mach numbers. After the optimum values of α, τ, and f_s were obtained by use of a fuselage skin drag coefficient of 0.0015 and equation (B3) for all Mach numbers, the final range parameter R/B was determined. The more exact value of fuselage skin friction drag coefficient calculated according to equation (B1) and the variation of body pressure drag with Mach number described in appendix B were used in the determination of R/B.

Solution of equations. - The solution of the analysis for any one set of conditions (one fuel density, Mach number, and altitude) consisted of satisfying the four equations (D2), (D8), (D9), and (D10) with the four variables w_f, α, τ, and f_s, with use of plots like those illustrated in figures 5 to 7. The correct wing, engine, and fuselage performance at these optimum conditions was then obtained and this performance substituted in equation (D3) to obtain the range parameter R/B.

The most convenient method of solving the four simultaneous equations was as follows: Approximate values of α, w_f, and τ were chosen. From a plot such as figure 5, $\frac{dD_w}{dw_w}$ was measured at the value of w_w corresponding to the assumed α. With equation (D11), $\frac{d\left(D_s \frac{10^3}{q_0}\right)}{dw_s}$ was calculated and an approximate f_s was obtained by using this slope in a curve such as figure 7. Values of D_w, w_w, U, D_s, and w_s corresponding to the approximate α, τ, and f_s were used and a new w_f was obtained from equation (D2).

A new τ was obtained from equation (D9) and a plot such as figure 6; a new α was obtained from equation (D8) and a plot like figure 5. If the new values differed substantially from the values originally assumed, the process was repeated with the new values. After accumulating a little experience in making the original approximations, it was seldom necessary to repeat the process more than once. The values of α, τ, f_s, and w_f obtained from this process were used to recalculate fuel weight w_f from equation (D2) with the more exact value of fuselage skin friction drag coefficient supplied by equation (B1) and the more exact variation of body pressure drag with Mach number as described in appendix B. The result was compared with the fuel weight obtained previously, and if necessary, this calculation was repeated with the corrected value of fuel weight, but this was necessary only in a few cases.

Numerical accuracy. - In general, the numerical accuracy of the calculations was held to three significant figures, but the use of plots for so large a portion of the calculations jeopardized this accuracy somewhat. The final values of range are probably within 3 percent, but the optimum values of α, τ, and f_s listed in table I may be off as much as 10 percent in some cases.

REFERENCES

1. Schamberg, R.: Effects of Flight Speed and Propulsive System on Aircraft Range. Rept. R-114, The Rand Corp., Aug. 13, 1948. (USAF Proj. MX-791, Proj. RAND.)

2. Keenan, Joseph H., and Kaye, Joseph: Gas Tables. John Wiley & Sons, Inc. (New York), 1948.

3. Jones, Robert T.: Estimated Lift-Drag Ratios at Supersonic Speed. NACA TN 1350, 1947.

4. Chemical Research Division Staff: Physical Properties and Thermodynamic Functions of Fuels, Oxidizers, and Products of Combustion. I - Fuels. Rep. R-127, Battelle Memorial Institute, The Rand Corp., Jan. 1949. (USAF contract W33-038 ac - 14105, Proj. RAND.)

5. Marks, Lionel S.: Mechanical Engineer's Handbook. 4th ed., McGraw-Hill Book Co., Inc., 1941.

6. Lippincott, Samuel B., and Lyman, Margaret M.: Vapor Pressure-Temperature Nomographs. Ind. and Eng. Chem., vol. 38, no. 3, March 1946, pp. 320-323.

7. Huff, Vearl N., and Gordon, Sanford: Tables of Thermodynamic Functions for Analysis of Aircraft-Propulsion Systems. NACA TN 2161, 1950.

8. von Kármán, Theodor, and Moore, Norton B.: Resistance of Slender Bodies Moving with Supersonic Velocities, with Special Reference to Projectiles. Trans. A.S.M.E., vol. 54, no. 23, December 15, 1932, pp. 303-310.

9. Tucker, Maurice: Approximate Calculation of Turbulent Boundary-Layer Development in Compressible Flow. NACA TN 2337, 1951.

10. Puckett, A. E., and Stewart, H. J.: Aerodynamic Performance of Delta Wings at Supersonic Speeds. Jour. Aero. Sci., vol. 14, no. 10, Oct. 1947, pp. 567-576.

11. Beane, Beverly: The Characteristics of Supersonic Wings Having Biconvex Sections. Jour. Aero. Sci., vol. 18, no. 1, Jan. 1951, pp. 7-20.

12. Stewart, H. J.: The Lift of a Delta Wing at Supersonic Speeds. Quarterly Appl. Math., vol. IV, no. 3, Oct. 1946, pp. 246-254.

13. Haack, W.: Projectile Shapes of Minimum Pressure Drag. Trans. CGD 253, Goodyear Aircraft Corp.

14. Cleveland Laboratory Staff: Performance and Ranges of Application of Various Types of Aircraft-Propulsion System. NACA TN 1349, 1947.

15. Taylor, G. I., and Maccoll, J. W.: The Air Pressure on a Cone Moving at High Speeds. - I. Proc. Roy. Soc. (London), ser. A, vol. 139, no. 383, Feb. 1, 1933, pp. 278-311.

16. Pinkel, I. Irving, and Shames, Harold: Analysis of Jet-Propulsion-Engine Combustion-Chamber Pressure Losses. NACA Rep. 880, 1947. (Formerly NACA TN 1180.)

2337

TABLE I - SUMMARY OF EFFECT OF FUEL DENSITY ON AIRCRAFT PERFORMANCE AT MAXIMUM RANGE; INITIAL GROSS WEIGHT, 150,000 POUNDS; PAY-LOAD AND CONTROLS WEIGHT, 10,000 POUNDS.

Mach number M_0	Fuel density ρ_f (lb/cu ft)	Angle of attack[a] α (radians)	Engine total-temperature ratio[a] τ	Fuselage fineness ratio[a] f_s	Wing loading (lb/sq ft)	Wing drag-lift ratio D_w	Wing weight to initial gross weight ratio w_w	Engine outlet area to combustion-chamber area ratio	Specific heat consumption K' (Btu/sec / lb thrust minus drag)	Number of engines	Fuselage diameter (ft)	Fuselage weight to initial gross weight ratio w_s	Airplane drag-lift ratio D_w+D_s	Fuel weight to initial gross weight ratio w_f	Range divided by effective heating value R/H (dimensionless)
Initial Altitude, 35,332 ft															
1.5	4	0.0678	4.59	13.5	170.3	0.1200	0.095	1.01	15.86	7.60	14.9	0.244	0.2274	0.544	0.407
	25	.0665	4.20	11.9	167.0	.1197	.096	.95	15.89	6.31	9.3	.144	.1683	.652	.733
	50	.0663	4.13	11.5	166.5	.1197	.096	.94	15.65	5.88	7.7	.123	.1537	.677	.880
	100	.0660	4.08	11.1	165.8	.1196	.096	.93	15.63	5.74	6.8	.109	.1453	.697	.975
	200	.0659	4.05	10.8	165.5	.1195	.096	.93	15.62	5.61	5.8	.099	.1398	.709	1.037
2.0	4	0.0728	3.21	14.7	230.5	0.1247	0.085	1.15	11.18	4.83	14.7	0.271	0.2831	0.545	0.622
	25	.0687	3.02	13.2	217.5	.1236	.086	1.11	11.09	3.52	9.0	.162	.1890	.661	1.290
	50	.0680	2.99	12.7	215.3	.1234	.087	1.10	11.08	3.23	7.5	.139	.1712	.682	1.522
	100	.0674	2.98	12.3	213.4	.1233	.087	1.10	11.07	3.02	6.4	.123	.1590	.703	1.718
	200	.0670	2.97	12.0	212.1	.1232	.087	1.10	11.07	2.89	5.6	.113	.1514	.714	1.862
2.5	4	0.0774	2.76	15.2	289.6	0.1285	0.078	1.54	10.02	3.01	14.5	0.282	0.3436	0.553	0.731
	25	.0707	2.58	14.0	264.5	.1265	.080	1.47	9.92	2.00	8.8	.173	.2121	.680	1.632
	50	.0695	2.55	13.6	260.0	.1262	.081	1.46	9.90	1.87	7.4	.150	.1879	.689	1.961
	100	.0687	2.53	13.2	257.1	.1260	.081	1.45	9.89	1.73	6.3	.133	.1721	.707	2.204
	200	.0681	2.52	12.8	254.8	.1260	.081	1.45	9.89	1.65	5.5	.123	.1629	.716	2.439
3.0	4	0.0817	2.20	15.5	356.5	0.1322	0.072	1.84	10.01	2.62	14.4	0.286	0.4050	0.556	0.749
	25	.0724	2.13	14.4	315.9	.1289	.076	1.91	9.97	1.63	8.7	.176	.2371	.687	1.747
	50	.0709	2.11	14.1	309.4	.1286	.076	1.90	9.97	1.44	7.3	.155	.2055	.691	2.156
	100	.0698	2.10	13.8	304.6	.1282	.077	1.89	9.97	1.31	6.2	.140	.1852	.708	2.474
	200	.0689	2.10	13.5	300.7	.1281	.077	1.88	9.97	1.23	5.4	.130	.1752	.717	2.732
3.5	4	0.0852	2.10	15.6	426.9	0.1350	0.068	2.23	10.63	2.31	14.3	0.285	0.4892	0.561	0.709
	25	.0736	2.03	14.8	368.8	.1306	.072	2.19	10.82	1.37	8.6	.181	.2597	.689	1.727
	50	.0719	2.02	14.5	360.3	.1302	.072	2.18	10.82	1.18	7.2	.159	.2223	.692	2.145
	100	.0705	2.02	14.3	353.2	.1298	.073	2.18	10.82	1.05	6.1	.144	.1973	.708	2.517
	200	.0695	2.01	14.0	348.2	.1297	.073	2.18	10.82	.96	5.3	.134	.1826	.718	2.806
4.0	4	0.0880	2.32	15.7	498.7	0.1365	0.065	2.82	12.55	1.72	14.2	0.282	0.5283	0.571	0.636
	25	.0743	2.25	15.1	421.1	.1314	.068	2.77	12.54	.99	8.6	.184	.2817	.672	1.583
	50	.0724	2.23	14.9	410.3	.1308	.069	2.75	12.54	.84	7.1	.162	.2565	.690	2.004
	100	.0709	2.22	14.7	401.8	.1304	.070	2.74	12.54	.74	6.0	.146	.2072	.711	2.383
	200	.0699	2.22	14.5	395.0	.1302	.070	2.74	12.54	.68	5.3	.137	.1905	.720	2.654
Initial Altitude, 50,000 ft															
1.5	4	0.0715	4.98	12.3	89.09	0.1225	0.126	1.06	16.33	11.7	15.0	0.211	0.1829	0.523	0.464
	25	.0705	4.71	10.6	87.85	.1225	.126	1.02	16.17	10.2	9.4	.119	.1498	.623	.753
	50	.0702	4.68	10.1	87.47	.1222	.126	1.01	16.16	9.89	7.9	.100	.1429	.644	.838
	100	.0699	4.64	9.7	87.10	.1221	.126	1.01	16.15	9.58	6.8	.090	.1382	.656	.902
	200	.0698	4.62	9.4	86.75	.1220	.126	1.01	16.12	9.41	6.0	.078	.1350	.668	.949
2.0	4	0.0748	3.13	15.4	117.5	0.1267	0.111	1.13	11.26	7.85	14.9	0.239	0.2180	0.535	0.779
	25	.0721	2.99	11.7	115.3	.1258	.112	1.10	11.23	6.29	9.2	.136	.1646	.643	1.391
	50	.0716	2.98	11.2	112.5	.1257	.113	1.10	11.23	5.97	7.7	.116	.1543	.664	1.572
	100	.0711	2.97	10.9	111.7	.1256	.113	1.10	11.23	5.77	6.8	.103	.1471	.678	1.717
	200	.0707	2.97	10.5	111.1	.1256	.113	1.10	11.23	5.68	5.8	.095	.1430	.690	1.820
2.5	4	0.0778	2.55	15.9	144.4	0.1301	0.102	1.46	10.00	5.09	14.8	0.251	0.3521	0.544	0.972
	25	.0735	2.47	12.6	136.4	.1288	.104	1.43	9.98	3.83	9.1	.149	.1798	.653	1.840
	50	.0727	2.46	12.1	134.9	.1286	.104	1.43	9.97	3.55	7.8	.128	.1614	.678	2.152
	100	.0721	2.45	11.7	133.8	.1285	.105	1.42	9.97	3.38	6.5	.114	.1584	.690	2.344
	200	.0717	2.45	11.3	133.1	.1283	.105	1.42	9.97	3.25	5.7	.105	.1505	.702	2.518
3.0	4	.0805	2.25	14.3	174.3	.1332	0.094	1.87	10.13	3.61	14.7	0.260	0.2879	0.551	1.028
	25	.0748	2.16	13.0	161.9	.1313	.097	1.92	10.09	2.62	9.0	.156	.1948	.680	2.056
	50	.0737	2.15	12.7	159.5	.1310	.098	1.92	10.08	2.40	7.5	.137	.1764	.679	2.390
	100	.0730	2.15	12.3	158.0	.1308	.098	1.92	10.08	2.24	6.4	.121	.1649	.697	2.687
	200	.0723	2.15	12.0	156.5	.1307	.098	1.92	10.08	2.14	5.6	.112	.1577	.702	2.880
3.5	4	0.0830	2.20	14.5	200.4	0.1352	0.088	2.29	10.94	2.97	14.6	0.263	0.3239	0.558	1.006
	25	.0757	2.12	13.4	186.2	.1327	.091	2.24	10.92	2.05	8.9	.162	.2084	.684	2.094
	50	.0745	2.11	13.1	183.2	.1324	.092	2.24	10.92	1.85	7.4	.141	.1864	.685	2.479
	100	.0735	2.11	12.8	182.7	.1322	.092	2.24	10.92	1.71	6.3	.127	.1724	.700	2.794
	200	.0728	2.11	12.5	181.0	.1320	.093	2.24	10.92	1.62	5.5	.117	.1638	.710	3.024
4.0	4	0.0850	2.30	14.7	259.0	0.1367	0.084	2.81	12.63	2.44	14.5	0.264	0.3568	0.564	0.970
	25	.0763	2.22	13.7	214.5	.1335	.087	2.74	12.60	1.61	8.8	.164	.2317	.668	1.971
	50	.0750	2.21	13.5	210.9	.1332	.088	2.73	12.60	1.44	7.3	.144	.1914	.689	2.369
	100	.0741	2.21	13.2	208.4	.1329	.088	2.73	12.60	1.32	6.2	.130	.1790	.704	2.696
	200	.0731	2.21	13.0	206.5	.1328	.088	2.73	12.60	1.24	5.5	.120	.1695	.715	2.951

[a]Optimum with respect to range.

[redacted]

TABLE I - SUMMARY OF EFFECT OF FUEL DENSITY ON AIRCRAFT PERFORMANCE AT MAXIMUM RANGE; INITIAL GROSS WEIGHT, 150,000 POUNDS; PAY-LOAD AND CONTROLS WEIGHT, 10,000 POUNDS Concluded

NACA

Mach number M_0	Fuel density ρ_f (lb/cu ft)	Angle of attack[a] α (radians)	Engine total-temperature ratio[a] τ	Fuselage fineness ratio[a] f_s	Wing loading (lb/sq ft)	Wing drag-lift ratio D_w	Wing weight to initial gross weight ratio w_w	Engine outlet area to combustion-chamber area ratio	Specific heat consumption H' (Btu/sec / lb thrust minus drag)	Number of engines	Fuselage diameter (ft)	Fuselage weight to initial gross weight ratio w_s	Airplane drag-lift ratio D_w+D_s	Fuel weight to initial gross weight ratio w_f	Range divided by effective heating value R/B (dimensionless)
Initial Altitude, 70,000 ft															
1.5	4	0.0780	5.70	10.7	37.41	0.1281	0.190	1.14	17.25	22.5	15.0	0.165	0.1638	0.453	0.480
	25	.0770	5.60	8.8	36.98	.1257	.191	1.13	17.12	20.7	9.7	.088	.1398	.520	.672
	50	.0767	5.58	8.3	36.79	.1256	.191	1.13	17.09	20.3	8.7	.078	.1365	.538	.818
	100	.0763	5.58	7.8	36.59	.1255	.192	1.13	17.09	19.9	7.8	.068	.1343	.549	.851
	200	.0760	5.58	7.5	36.48	.1249	.194	1.13	17.12	19.6	7.4	.063	.1325	.557	.873
2.0	4	0.0797	5.40	11.7	48.20	0.1300	0.187	1.19	11.57	14.4	15.1	0.194	0.1710	0.476	0.617
	25	.0780	5.30	9.8	47.17	.1294	.188	1.17	11.53	13.1	9.7	.105	.1490	.572	1.235
	50	.0776	5.28	9.3	46.93	.1293	.189	1.17	11.53	12.1	8.6	.087	.1447	.592	1.345
	100	.0773	5.28	9.0	46.75	.1292	.189	1.17	11.53	11.8	7.8	.077	.1406	.604	1.429
	200	.0770	5.28	8.8	46.66	.1291	.190	1.17	11.53	11.4	7.2	.068	.1367	.612	1.480
2.5	4	0.0812	2.65	12.2	58.01	0.1335	0.182	1.50	10.19	9.49	15.1	0.210	0.1899	0.504	1.153
	25	.0789	2.60	10.5	56.37	.1325	.184	1.48	10.17	8.15	9.8	.117	.1552	.603	1.782
	50	.0785	2.59	10.1	56.09	.1325	.185	1.48	10.16	7.88	8.6	.099	.1514	.624	1.985
	100	.0782	2.59	9.7	55.87	.1324	.185	1.48	10.16	7.65	7.7	.087	.1469	.637	2.111
	200	.0779	2.59	9.4	55.66	.1323	.185	1.48	10.16	7.50	7.1	.079	.1441	.646	2.217
3.0	4	0.0828	2.47	12.6	68.82	0.1359	0.181	2.08	10.39	5.87	15.0	0.221	0.2075	0.528	1.598
	25	.0797	2.36	11.1	66.40	.1348	.183	2.02	10.30	5.12	9.6	.127	.1682	.624	2.139
	50	.0792	2.33	10.7	65.98	.1346	.183	2.01	10.29	4.96	8.6	.108	.1577	.644	2.376
	100	.0788	2.33	10.3	65.66	.1345	.184	2.01	10.29	4.78	7.7	.096	.1521	.658	2.580
	200	.0785	2.33	10.0	65.40	.1344	.184	2.01	10.29	4.67	7.0	.087	.1486	.668	2.694
3.5	4	0.0838	2.44	12.9	80.27	0.1378	0.181	2.43	11.21	4.56	15.0	0.228	0.2256	0.537	1.930
	25	.0805	2.33	11.5	77.02	.1366	.183	2.37	11.13	3.78	9.6	.133	.1742	.637	2.578
	50	.0800	2.32	11.1	76.54	.1364	.184	2.36	11.12	3.58	8.4	.114	.1638	.656	2.867
	100	.0795	2.32	10.8	76.06	.1362	.184	2.36	11.12	3.43	7.6	.102	.1568	.669	2.781
	200	.0792	2.32	10.5	75.78	.1362	.184	2.36	11.12	3.34	7.0	.095	.1527	.679	2.853
4.0	4	0.0851	2.43	13.2	92.04	0.1387	0.185	2.90	12.82	3.65	14.9	0.254	0.2407	0.543	1.958
	25	.0811	2.33	11.8	87.71	.1373	.186	2.85	12.74	3.19	9.4	.158	.1812	.642	2.888
	50	.0805	2.32	11.5	87.06	.1371	.186	2.82	12.73	2.99	8.4	.119	.1686	.653	2.836
	100	.0801	2.32	11.2	86.65	.1370	.186	2.82	12.73	2.84	7.5	.106	.1605	.677	2.782
	200	.0797	2.32	10.9	86.20	.1369	.187	2.82	12.73	2.76	6.9	.098	.1568	.685	2.892
Initial Altitude, 100,000 ft															
2.5	4	0.1030	4.50	9.8	17.55	0.1470	0.288	2.08	12.05	18.4	14.8	0.139	0.1640	0.371	0.733
	25	.0970	4.25	7.8	16.63	.1455	.296	2.01	11.80	17.2	9.5	.087	.1527	.456	.982
	50	.0964	4.13	7.4	16.43	.1450	.297	1.98	11.64	18.2	8.0	.055	.1502	.445	1.061
	100	.0961	4.05	7.1	16.58	.1425	.298	1.95	11.58	18.4	7.0	.047	.1463	.458	1.094
	200	.0960	4.00	6.8	16.36	.1425	.296	1.94	11.52	18.5	6.3	.042	.1475	.456	1.118
3.0	4	0.1046	3.86	10.2	20.80	0.1500	0.260	2.63	11.57	12.6	15.0	0.153	0.1721	0.416	1.011
	25	.0987	3.59	8.2	19.62	.1465	.269	2.55	11.40	12.4	9.6	.078	.1583	.487	1.364
	50	.0981	3.55	7.8	19.50	.1460	.270	2.53	11.36	12.2	8.1	.063	.1551	.500	1.473
	100	.0978	3.52	7.5	19.44	.1460	.271	2.52	11.32	12.2	7.0	.054	.1532	.508	1.533
	200	.0977	3.28	7.2	19.42	.1460	.271	2.50	11.28	12.3	6.3	.049	.1521	.512	1.564
3.5	4	0.1080	3.30	10.5	24.19	0.1520	0.239	2.94	12.25	10.1	15.1	0.164	0.1796	0.445	1.169
	25	.1000	3.13	8.6	22.82	.1485	.247	2.84	12.04	9.74	9.6	.085	.1627	.519	1.632
	50	.0994	3.10	8.1	22.69	.1480	.248	2.82	12.05	9.65	8.2	.070	.1592	.534	1.742
	100	.0991	3.07	7.8	22.62	.1480	.248	2.81	12.01	9.62	7.1	.061	.1568	.543	1.818
	200	.0990	3.04	7.5	22.59	.1480	.248	2.79	11.94	9.86	6.3	.053	.1554	.548	1.869
4.0	4	0.1069	3.36	11.0	27.60	0.1520	0.225	3.51	13.88	8.07	15.1	0.177	0.1838	0.461	1.209
	25	.1006	3.20	9.0	25.97	.1490	.230	3.42	13.73	7.67	9.6	.091	.1685	.544	1.727
	50	.0999	3.16	8.5	25.79	.1490	.231	3.40	13.69	7.62	8.1	.076	.1616	.559	1.848
	100	.0996	3.15	8.2	25.71	.1490	.231	3.38	13.66	7.59	7.0	.066	.1589	.569	1.936
	200	.0994	3.10	7.9	25.66	.1490	.231	3.38	13.62	7.62	6.2	.060	.1573	.574	1.987

[a]Optimum with respect to range.

TABLE II - WING WEIGHT FOR MINIMUM WING DRAG-LIFT RATIO. INITIAL GROSS WEIGHT, 150,000 POUNDS.

Altitude (ft)	Mach number M_O	Angle of attack for minimum wing drag-lift ratio (radians)	Minimum wing drag-lift ratio	Wing weight to initial gross weight ratio W_W
35,332	1.5	0.0596	0.1191	0.1001
35,332	2.0	.0613	.1225	.0903
35,332	2.5	.0626	.1252	.0841
35,332	3.0	.0637	.1276	.0791
35,332	3.5	.0645	.1290	.0750
35,332	4.0	.0647	.1294	.0718
50,000	1.5	.0602	.1204	.1350
50,000	2.0	.0621	.1241	.1199
50,000	2.5	.0635	.1270	.1104
50,000	3.0	.0647	.1297	.1028
50,000	3.5	.0656	.1311	.0967
50,000	4.0	.0659	.1318	.0920
70,000	1.5	.0611	.1221	.2152
70,000	2.0	.0631	.1262	.1875
70,000	2.5	.0648	.1296	.1701
70,000	3.0	.0660	.1320	.1560
70,000	3.5	.0668	.1335	.1454
70,000	4.0	.0672	.1347	.1369
100,000	2.5	.0668	.1335	.3694
100,000	3.0	.0682	.1364	.3325
100,000	3.5	.0691	.1382	.3040
100,000	4.0	.0695	.1390	.2823

TABLE III - ENGINE CHARACTERISTICS AT TEMPERATURE RATIO FOR MINIMUM SPECIFIC HEAT CONSUMPTION. COMBUSTION-CHAMBER CROSS-SECTION AREA, 10 SQUARE FEET.

Altitude (ft)	Mach number M_0	Total-temperature ratio for minimum specific heat consumption	Minimum specific heat consumption $\left(\frac{\text{Btu/sec}}{\text{lb thrust minus drag}}\right)$	Engine specific weight $\left(\frac{\text{lb engine}}{\text{lb thrust minus drag}}\right)$	Engine thrust minus nacelle drag (lb)
35,332	1.5	3.64	15.50	0.295	3200
35,332	2.0	2.80	11.03	.139	7150
35,332	2.5	2.41	9.88	.076	13,700
35,332	3.0	2.05	9.96	.056	20,200
35,332	3.5	2.04	10.81	.042	28,850
35,332	4.0	2.20	12.50	.030	41,200
50,000	1.5	3.64	15.80	.605	1570
50,000	2.0	2.83	11.20	.280	3600
50,000	2.5	2.40	9.97	.157	6650
50,000	3.0	2.05	10.07	.116	10,050
50,000	3.5	2.02	10.90	.086	13,800
50,000	4.0	2.16	12.59	.064	19,600
70,000	1.5	3.84	16.26	1.500	630
70,000	2.0	2.94	11.43	.695	1430
70,000	2.5	2.48	10.13	.393	2680
70,000	3.0	2.18	10.31	.269	4270
70,000	3.5	2.08	11.03	.213	5600
70,000	4.0	2.23	12.87	.159	7810
100,000	2.5	2.57	10.40	1.593	670
100,000	3.0	2.16	10.46	1.174	980
100,000	3.5	2.12	11.30	.883	1350
100,000	4.0	2.30	12.97	.646	1960

[redacted]

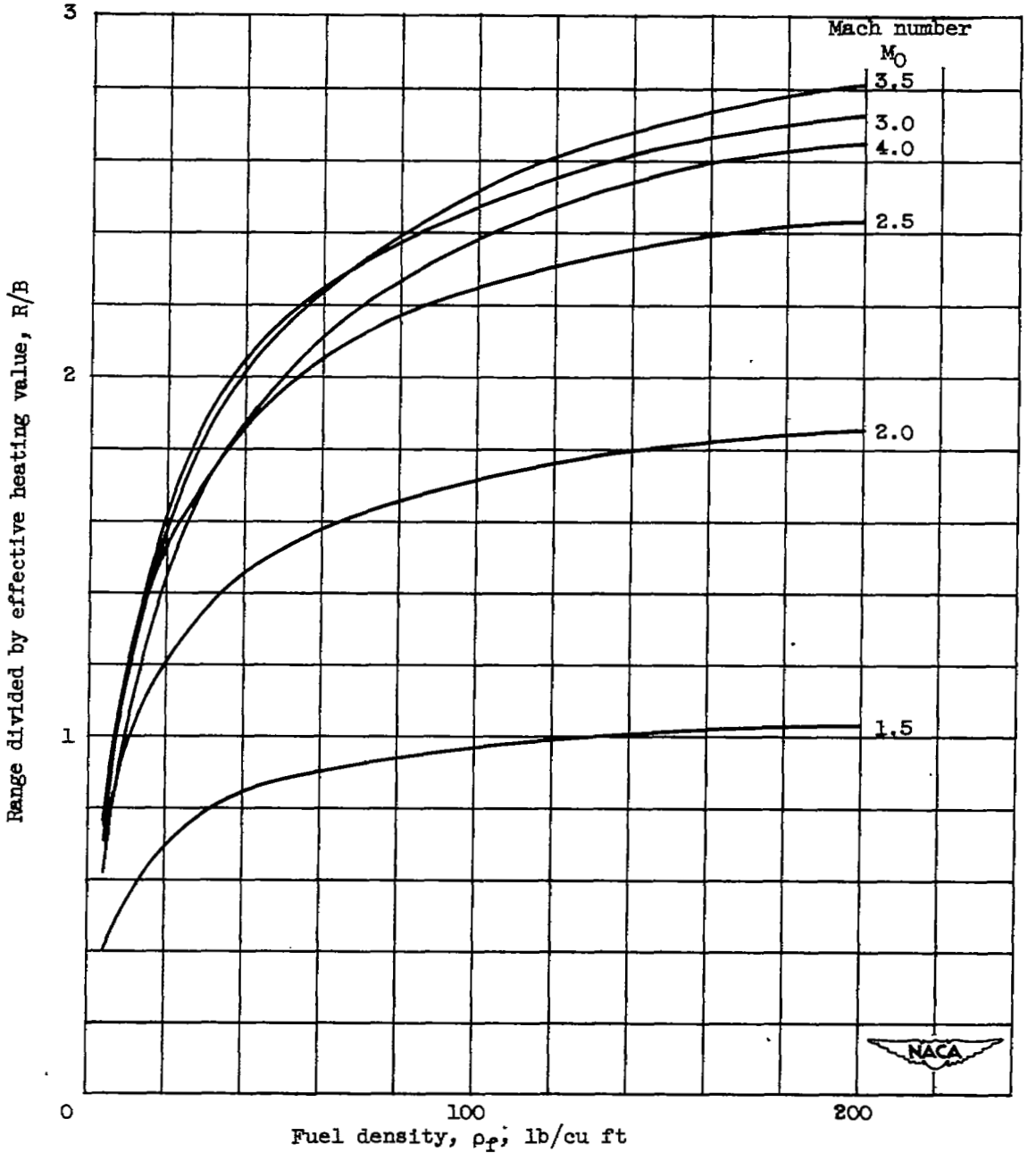

(a) Initial altitude, 35,332 feet.

Figure 1. - Effect of fuel density on range at various Mach numbers. Initial gross weight, 150,000 pounds; pay-load and controls weight, 10,000 pounds.

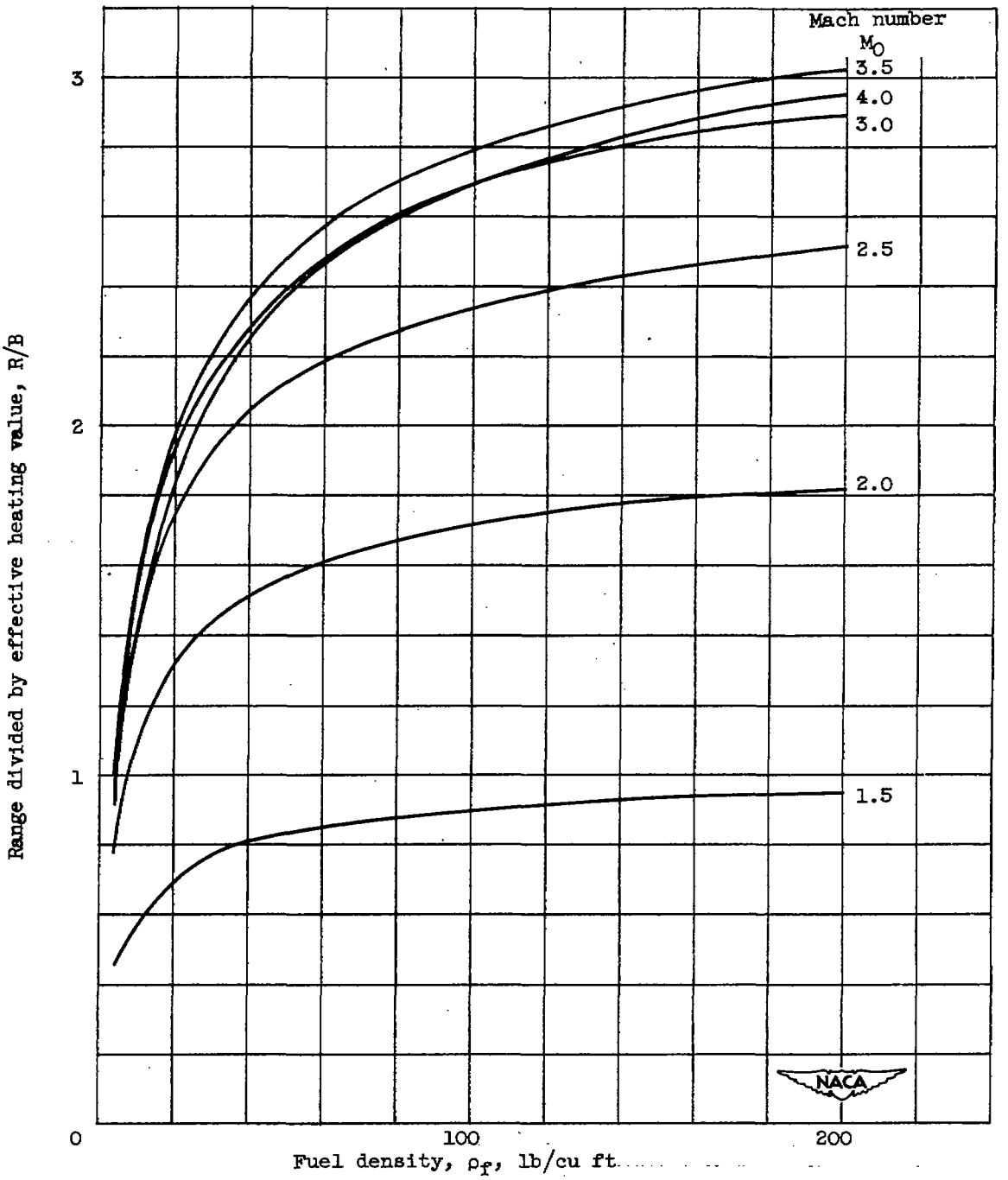

(b) Initial altitude, 50,000 feet.

Figure 1. - Continued. Effect of fuel density on range at various Mach numbers. Initial gross weight, 150,000 pounds; pay-load and controls weight, 10,000 pounds.

[redacted]

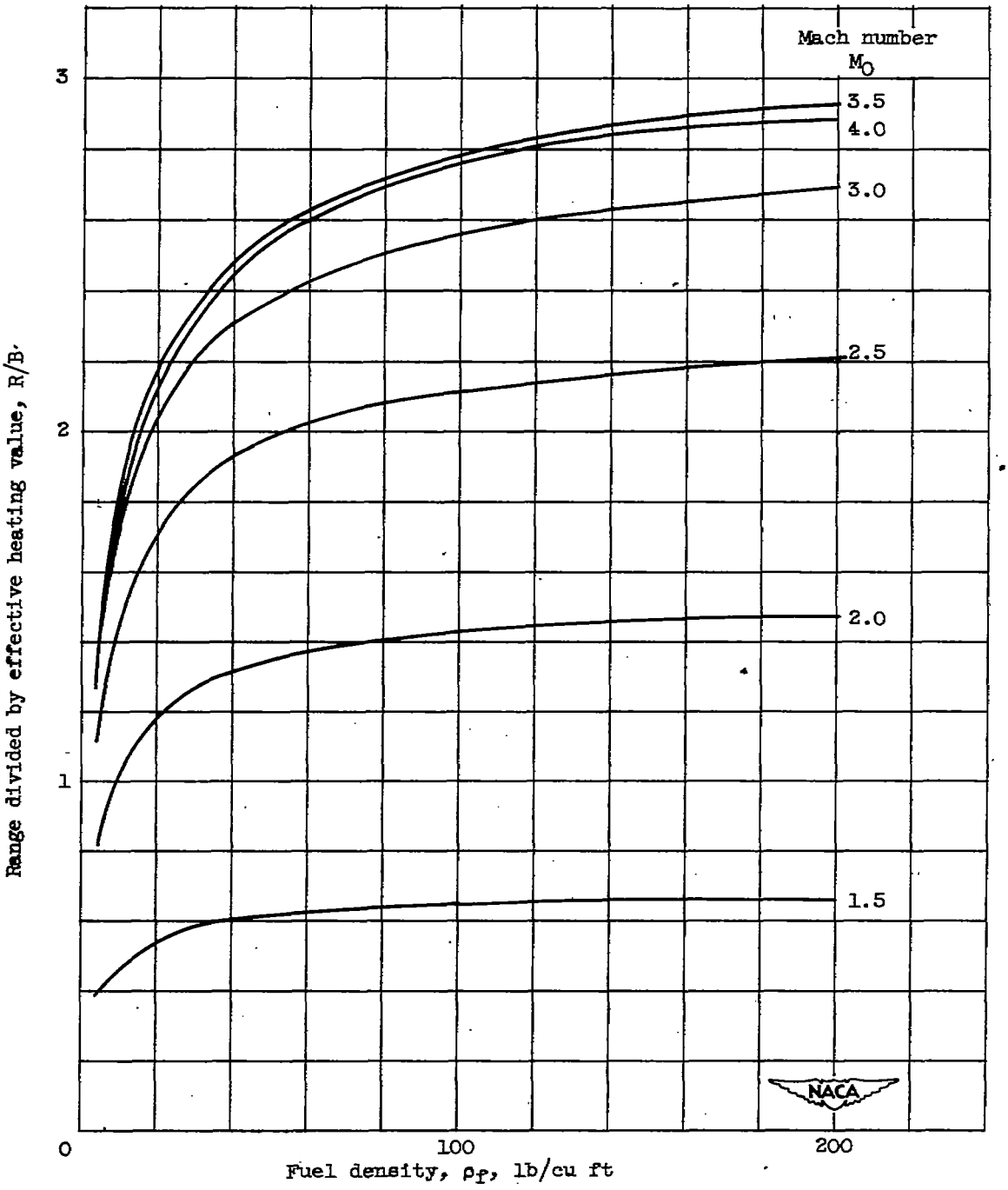

(c) Initial altitude, 70,000 feet.

Figure 1. - Continued. Effect of fuel density on range at various Mach numbers. Initial gross weight, 150,000 pounds; pay-load and controls weight, 10,000 pounds.

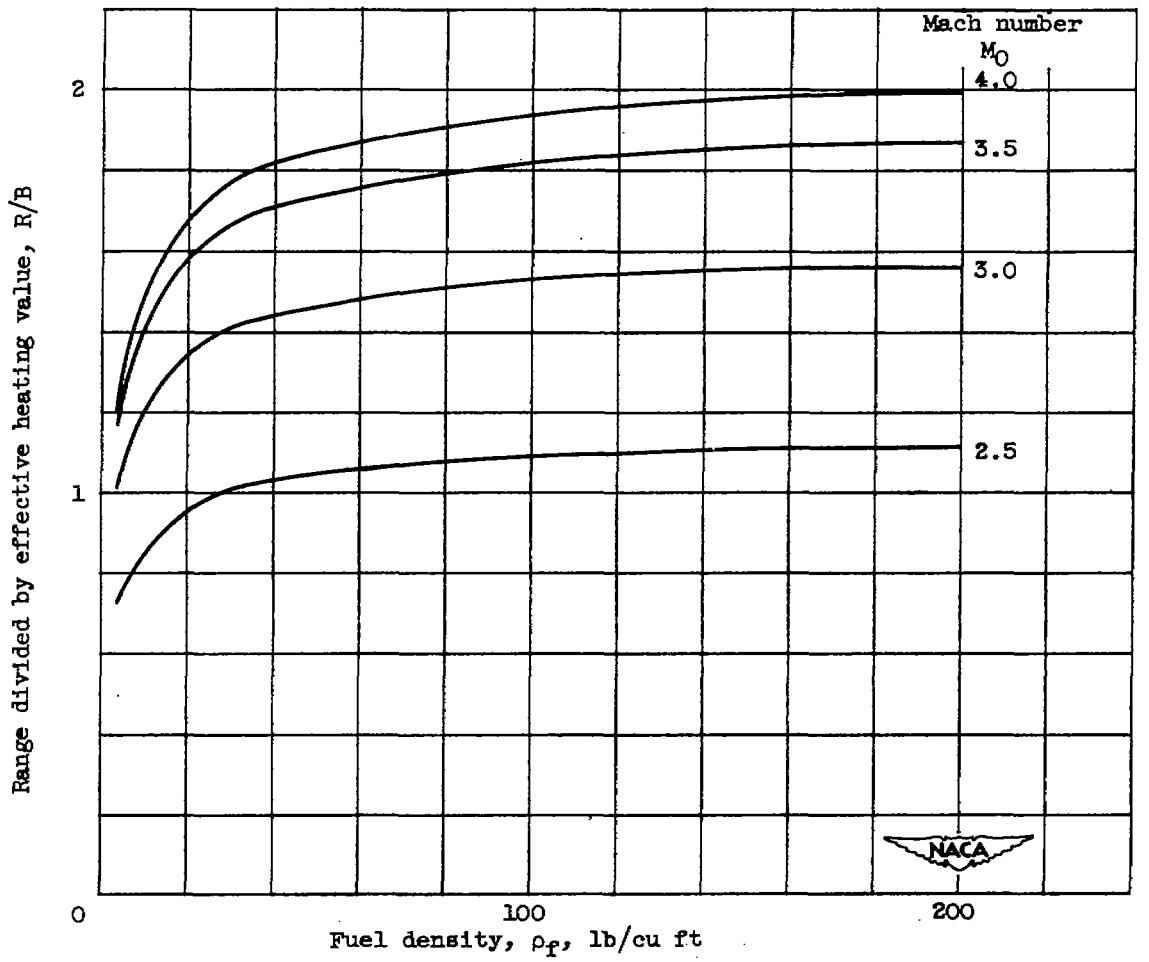

(d) Initial altitude, 100,000 feet.

Figure 1. - Concluded. Effect of fuel density on range at various Mach numbers. Initial gross weight, 150,000 pounds; pay-load and controls weight, 10,000 pounds.

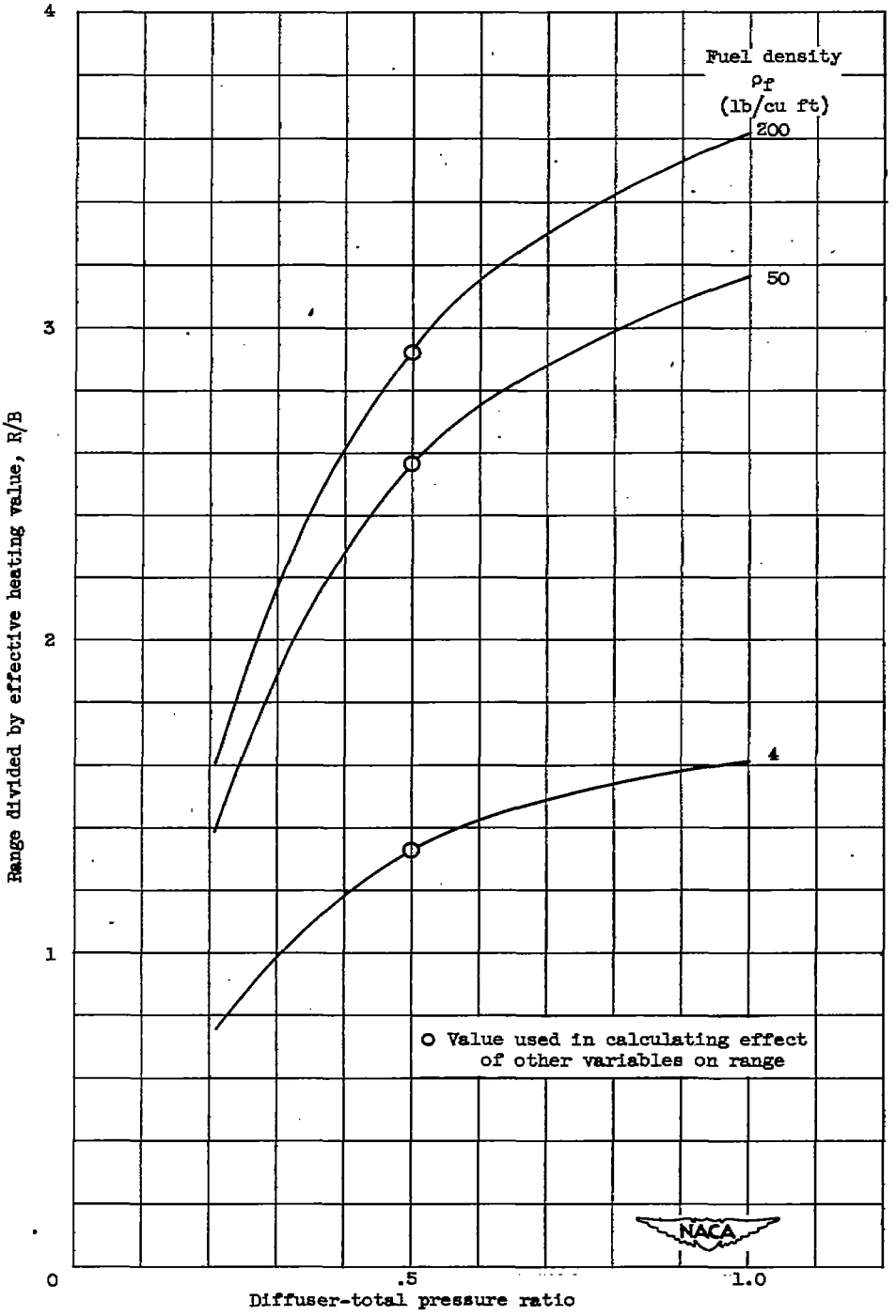

(a) Diffuser total-pressure ratio

Figure 2. - Effect of design variables on range for three fuel densities. Initial altitude, 70,000 feet; Mach number, 3.5; pay-load and controls weight, 10,000 pounds.

[redacted]

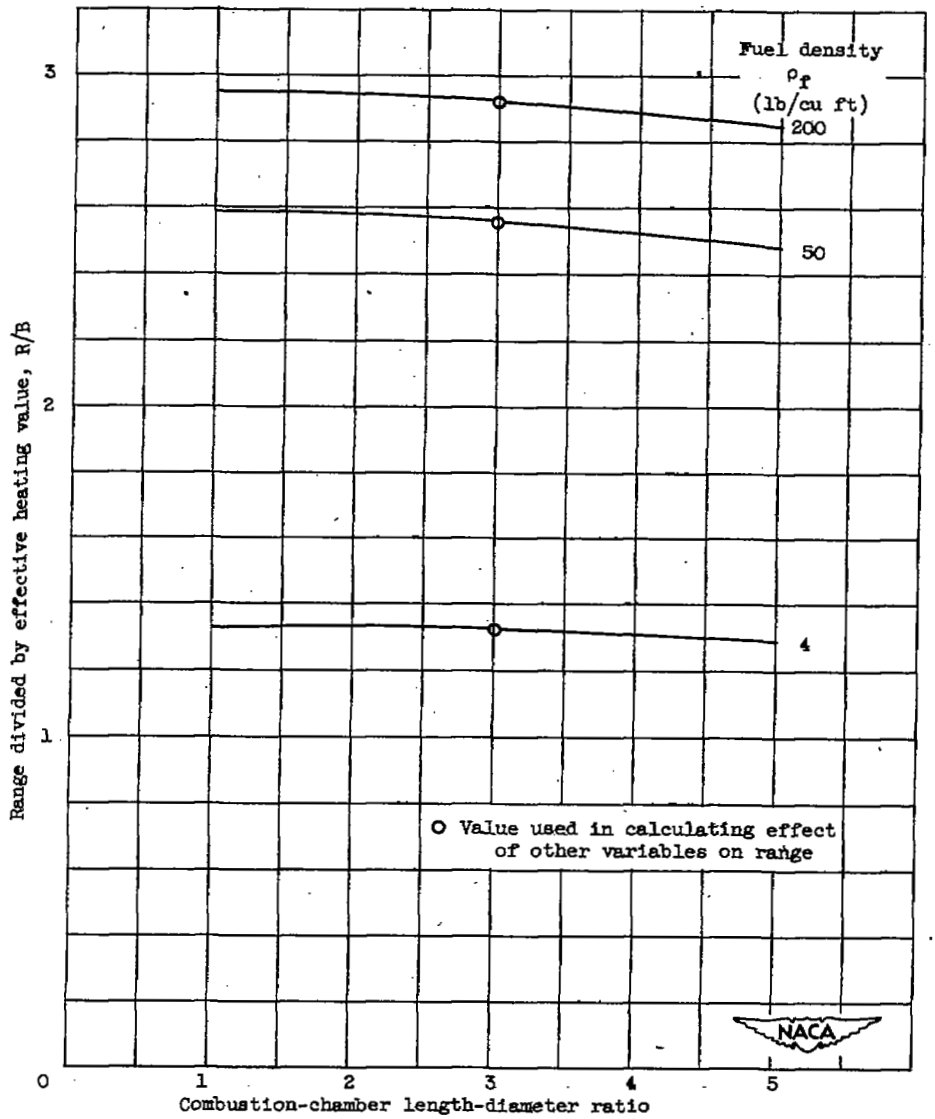

(b) Combustion-chamber length-diameter ratio.

Figure 2. - Continued. Effect of design variables on range for three fuel densities. Initial altitude, 70,000 feet; Mach number, 3.5; pay-load and controls weight, 10,000 pounds.

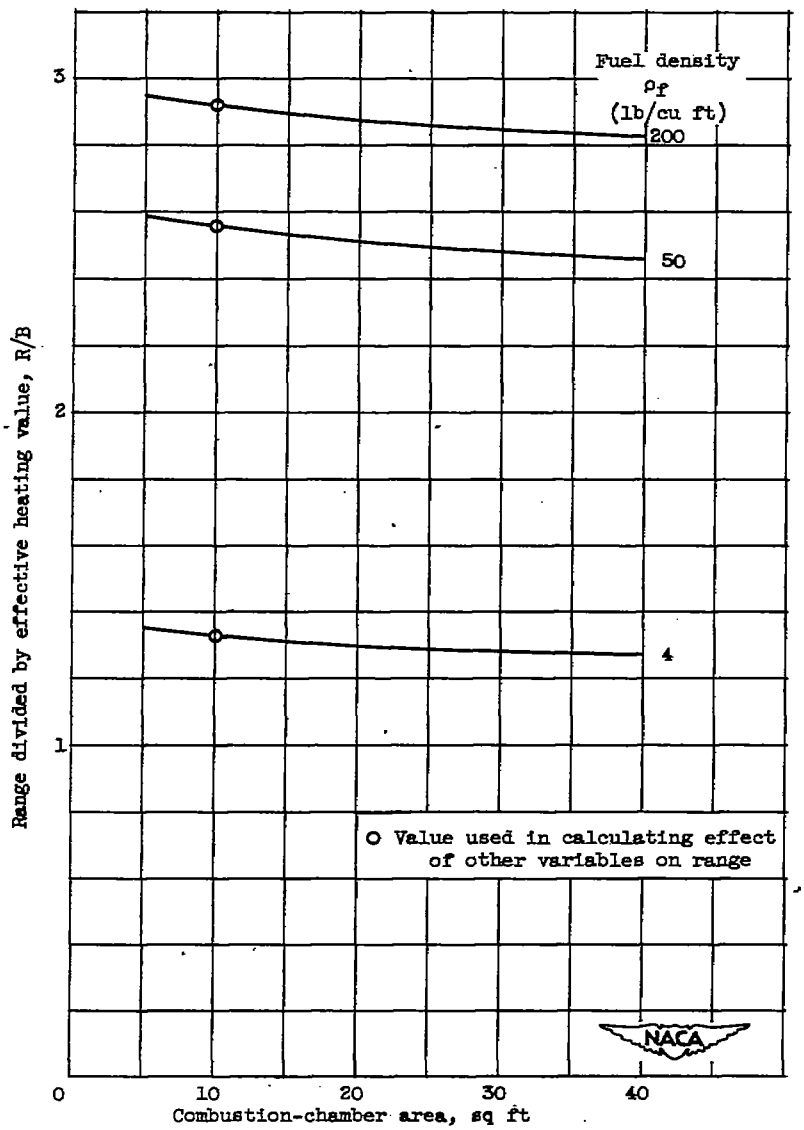

(c) Combustion-chamber area.

Figure 2. - Continued. Effect of design variables on range for three fuel densities. Initial altitude, 70,000 feet; Mach number, 3.5; pay-load and controls weight, 10,000 pounds.

[redacted]

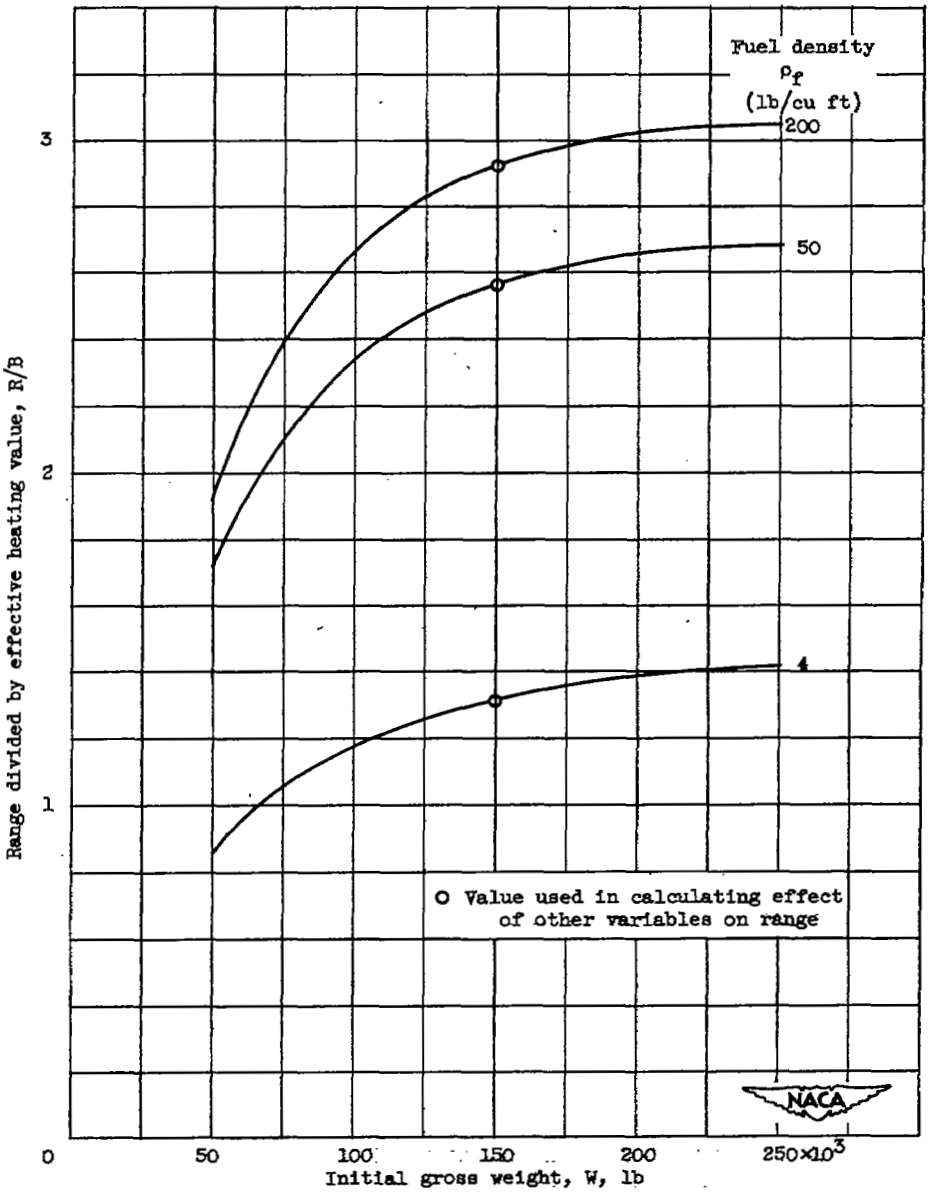

(d) Initial gross weight.

Figure 2. - Continued. Effect of design variables on range for three fuel densities. Initial altitude, 70,000 feet; Mach number, 3.5; pay-load and controls weight, 10,000 pounds.

[redacted]

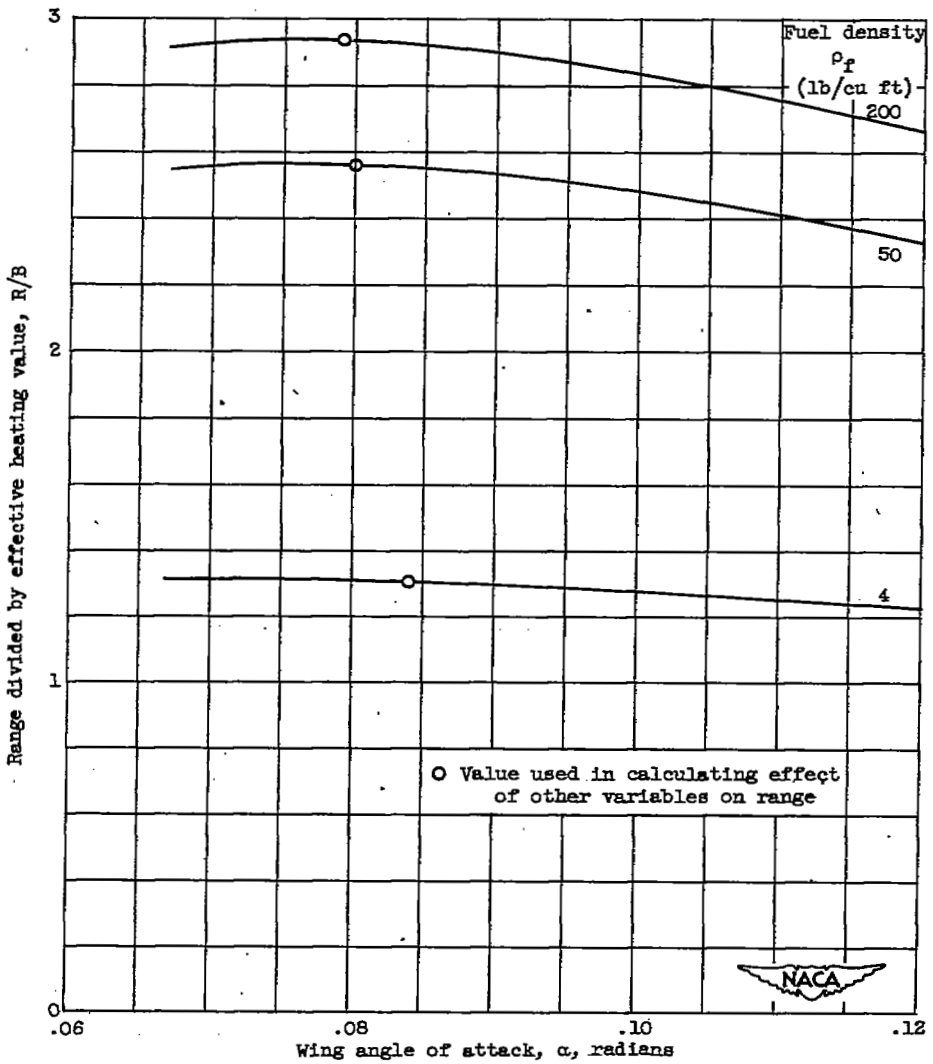

(e) Wing angle of attack.

Figure 2. - Continued. Effect of design variables on range for three fuel densities. Initial altitude, 70,000 feet; Mach number, 3.5; pay-load and controls weight, 10,000 pounds.

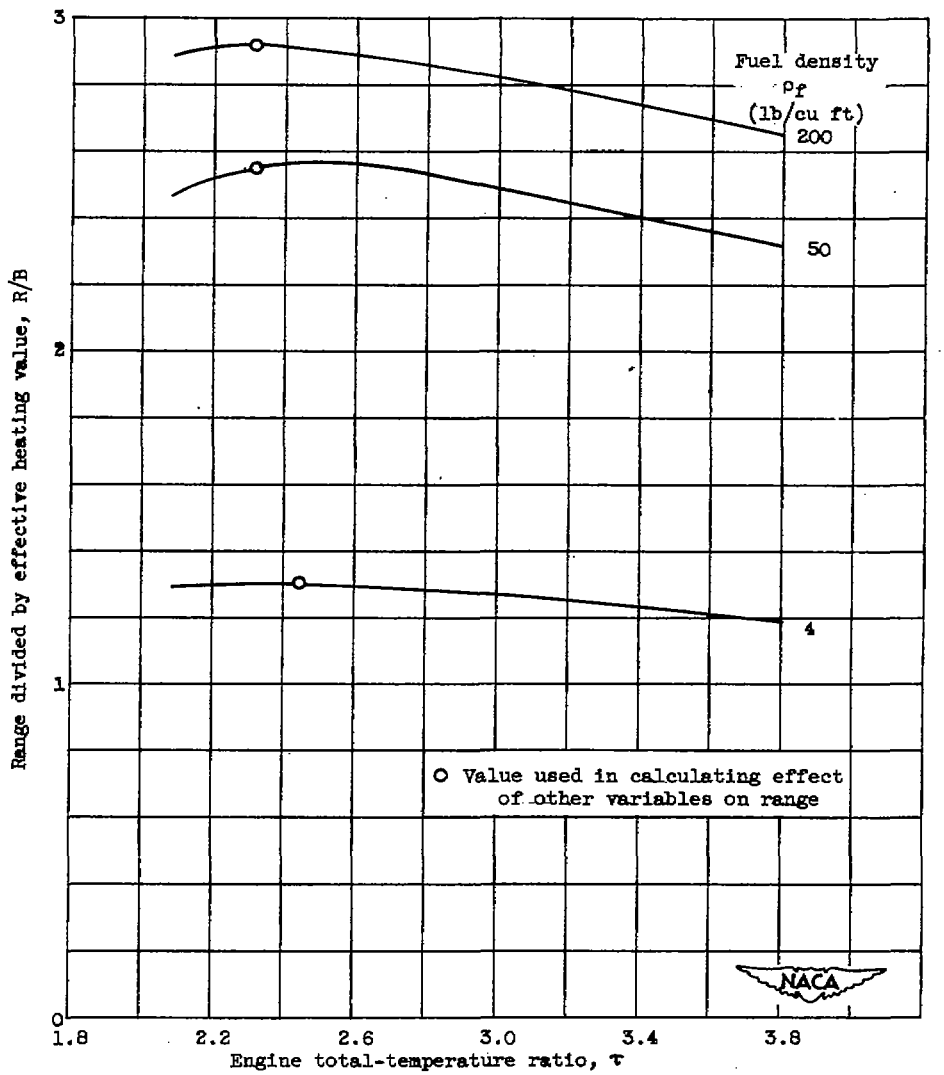

(f) Engine total-temperature ratio.

Figure 2. - Continued. Effect of design variables on range for three fuel densities. Initial altitude, 70,000 feet; Mach number, 3.5; pay-load and controls weight, 10,000 pounds.

2334

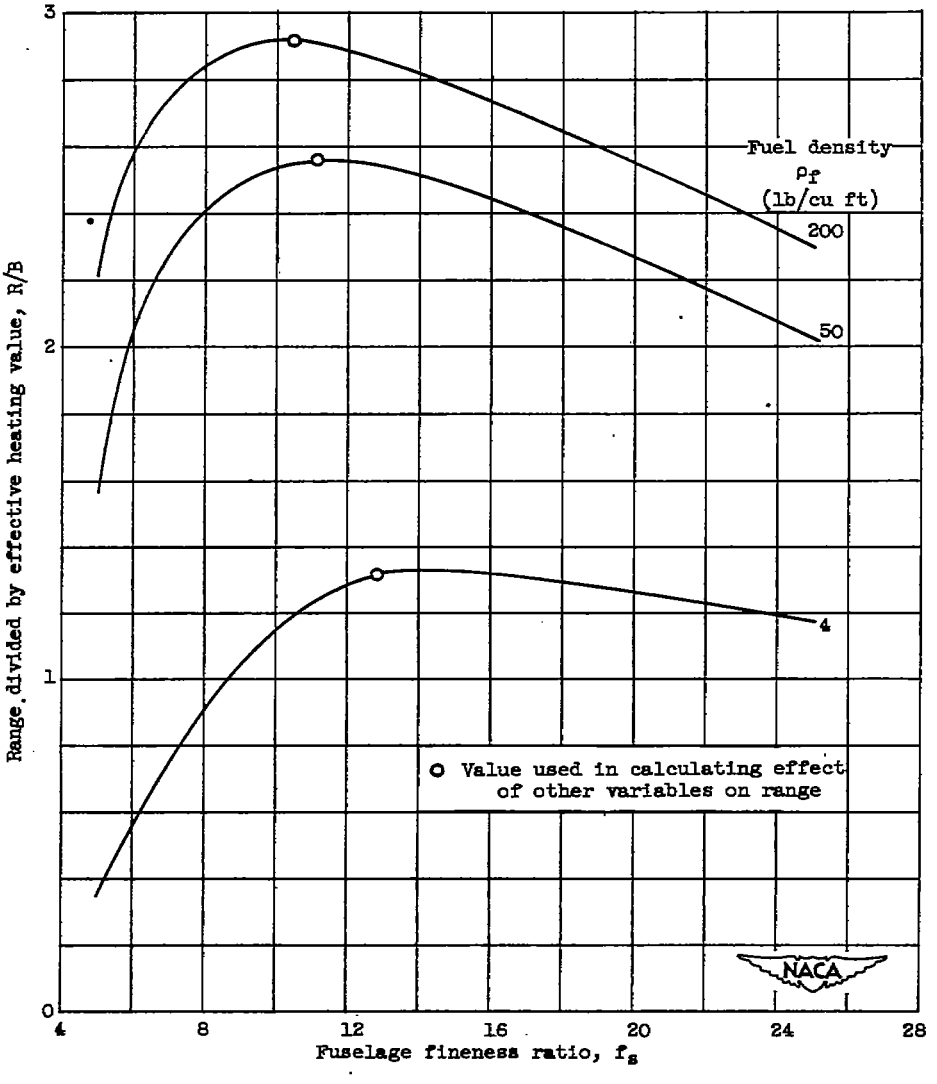

(g) Fuselage-fineness ratio.

Figure 2. - Concluded. Effect of design variables on range for three fuel densities. Initial altitude, 70,000 feet; Mach number, 3.5; pay-load and controls weight, 10,000 pounds.

[redacted]

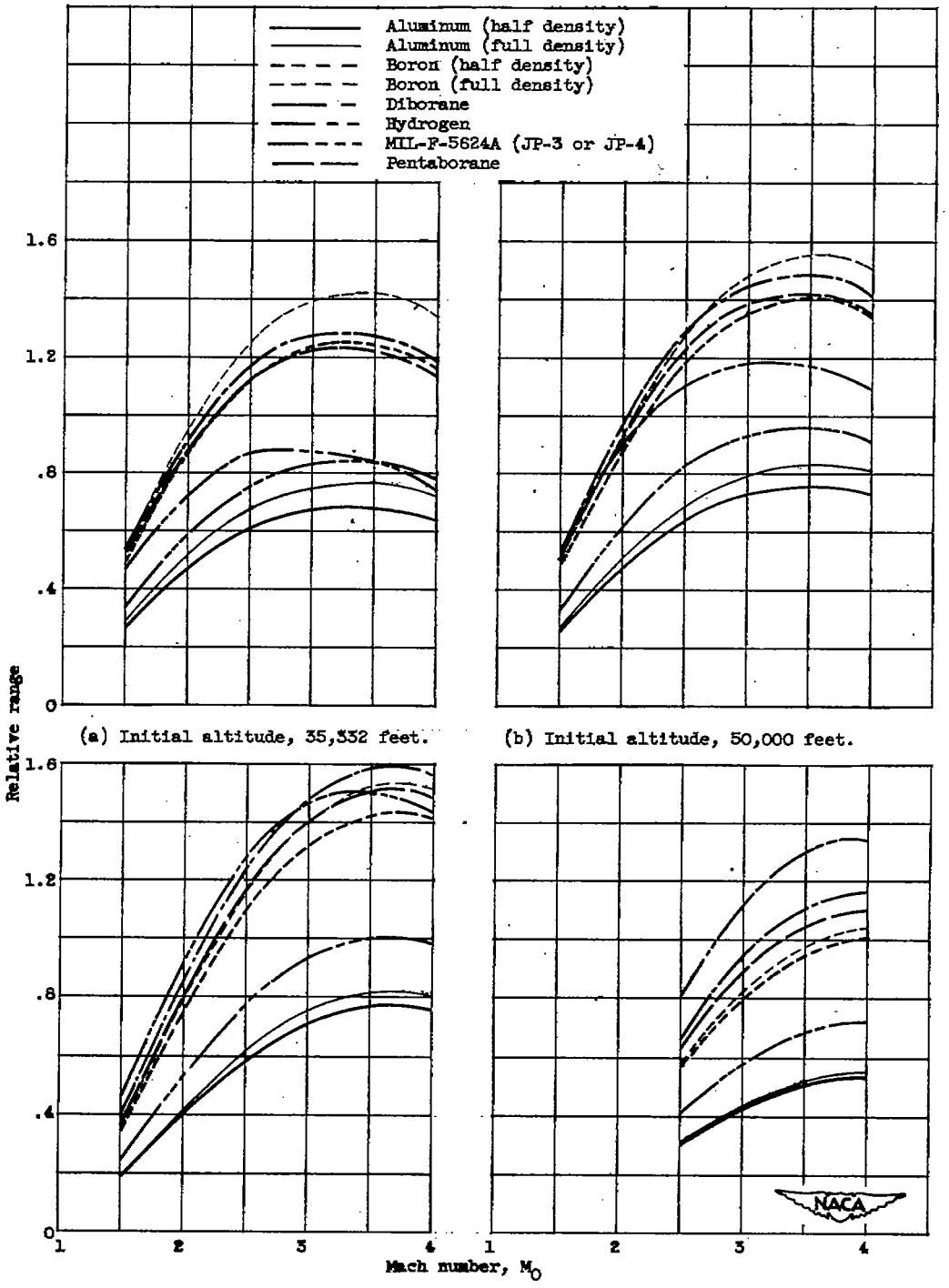

(a) Initial altitude, 35,332 feet.

(b) Initial altitude, 50,000 feet.

(c) Initial altitude, 70,000 feet.

(d) Initial altitude, 100,000 feet.

Figure 3. - Comparison of range potentialities of six ram-jet engine fuels. Initial gross weight, 150,000 pounds; pay-load and controls weight, 10,000 pounds.

[redacted]

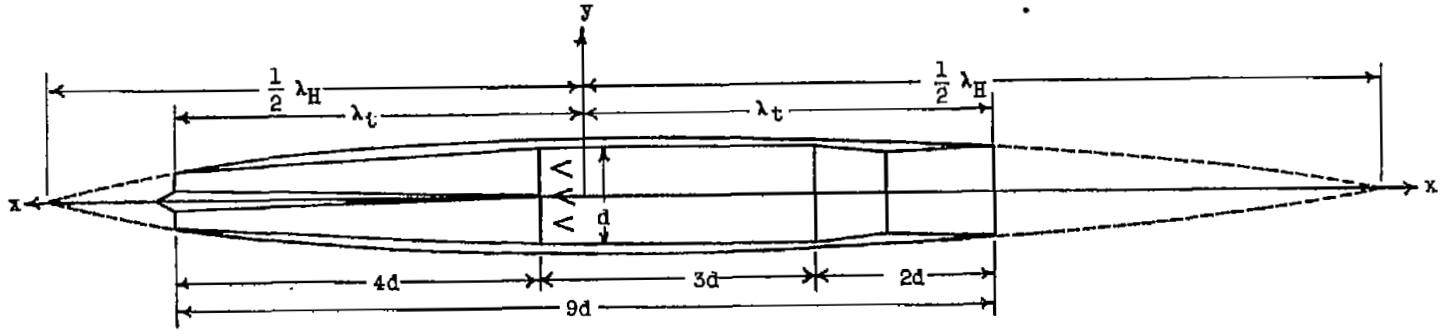

(a) Boattail nozzle.

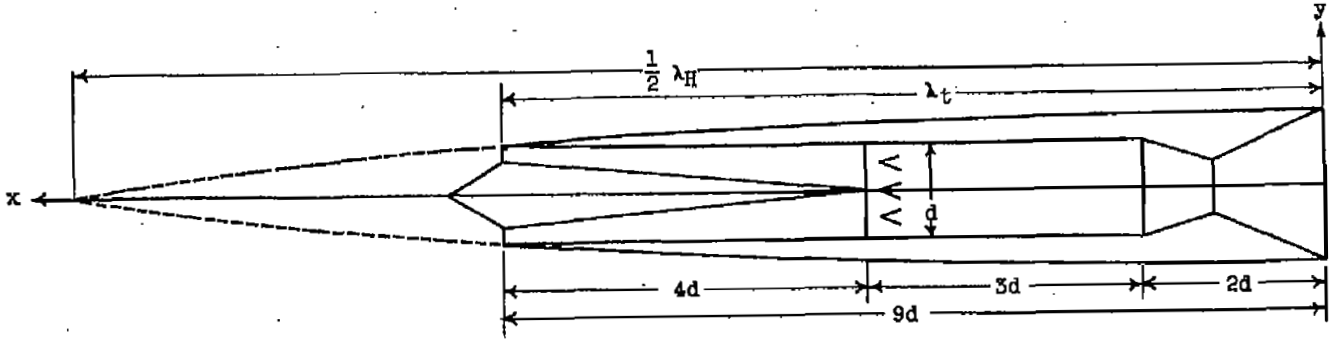

(b) Flare nozzle.

Figure 4. - Ram-jet engine geometry.

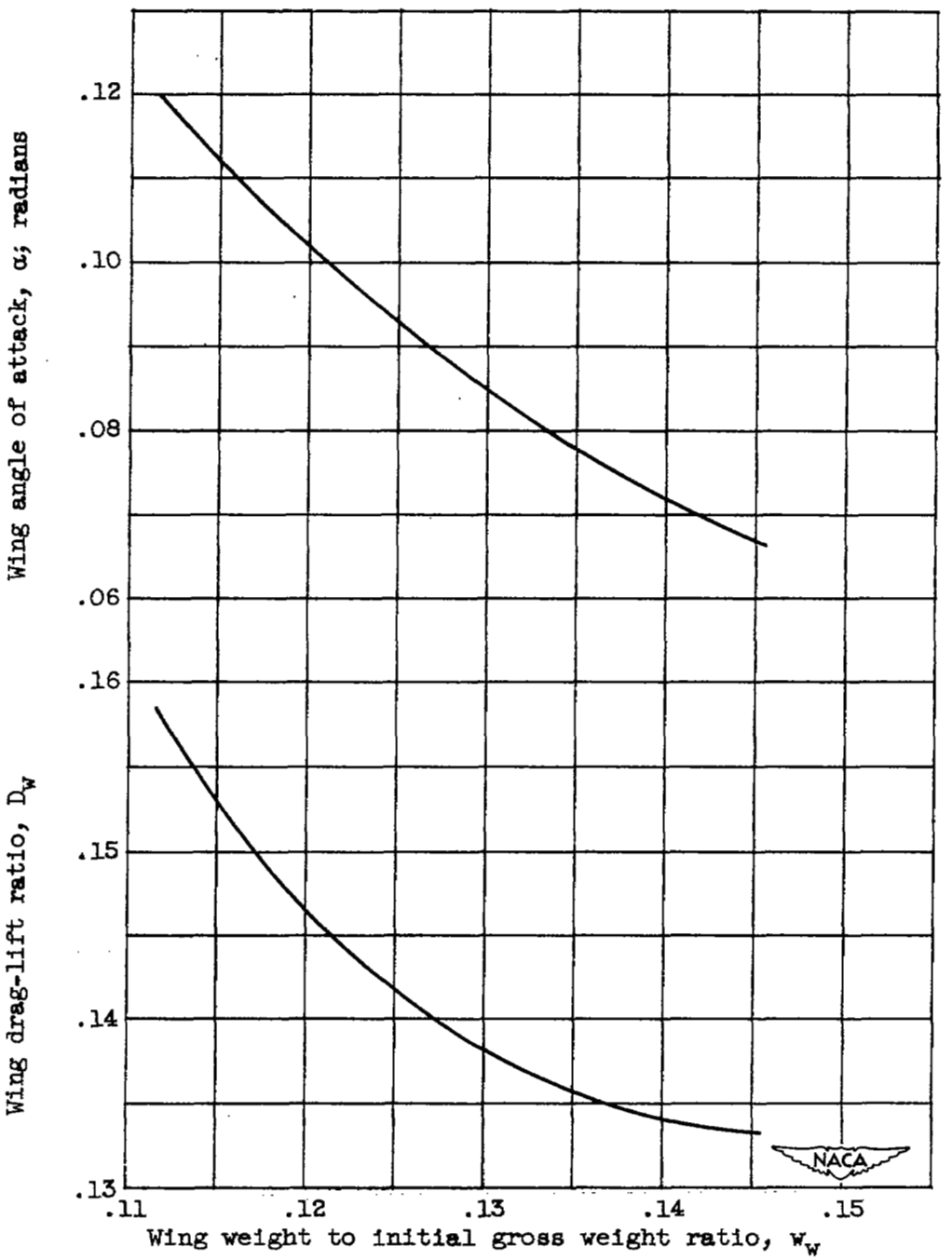

Figure 5. - Typical wing characteristics. Altitude, 70,000 feet; Mach number, 3.5; initial gross weight, 150,000 pounds.

[redacted]

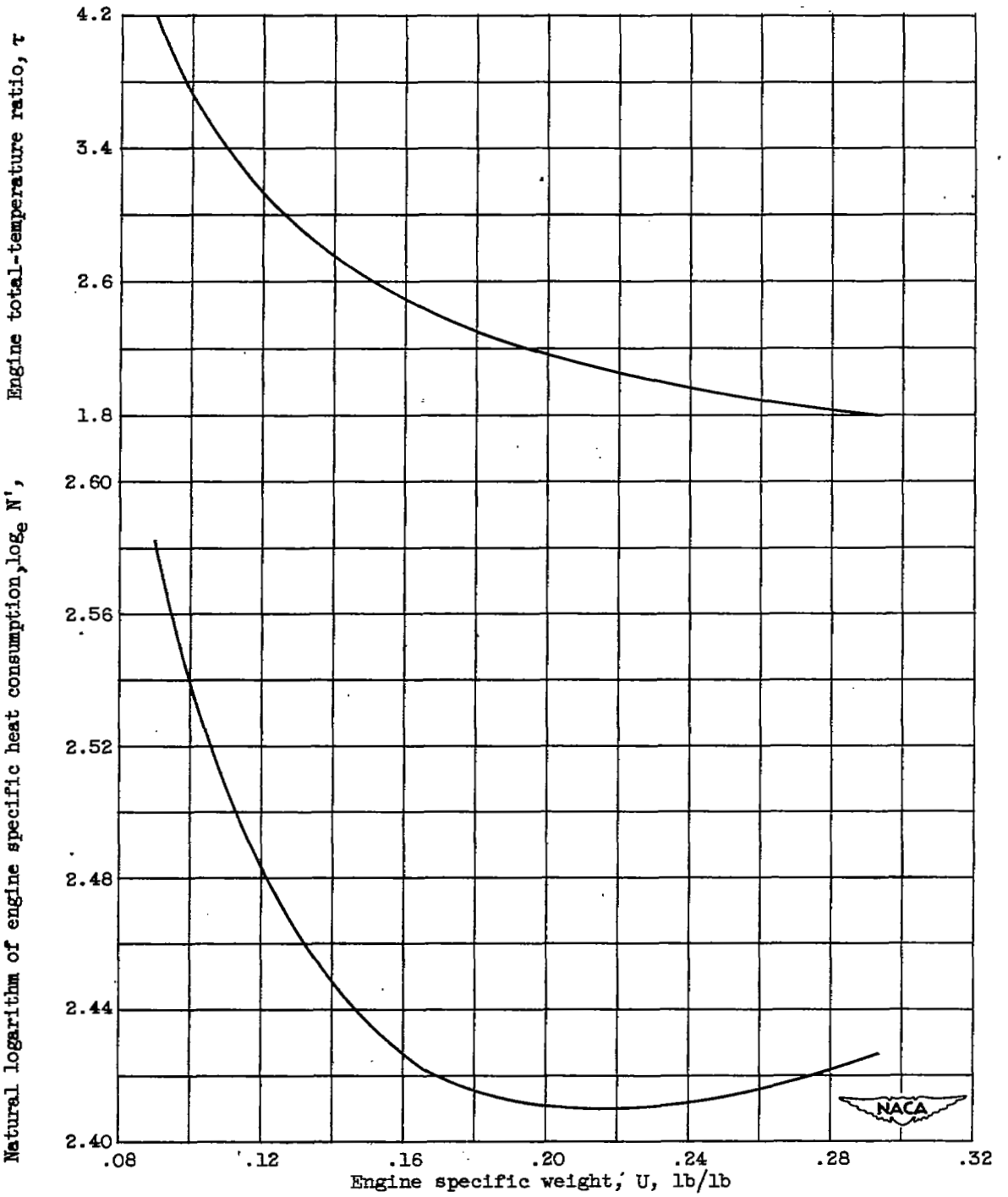

Figure 6. - Typical engine characteristics. Altitude, 70,000 feet; Mach number, 3.5; combustion-chamber cross-section area, 10 square feet.

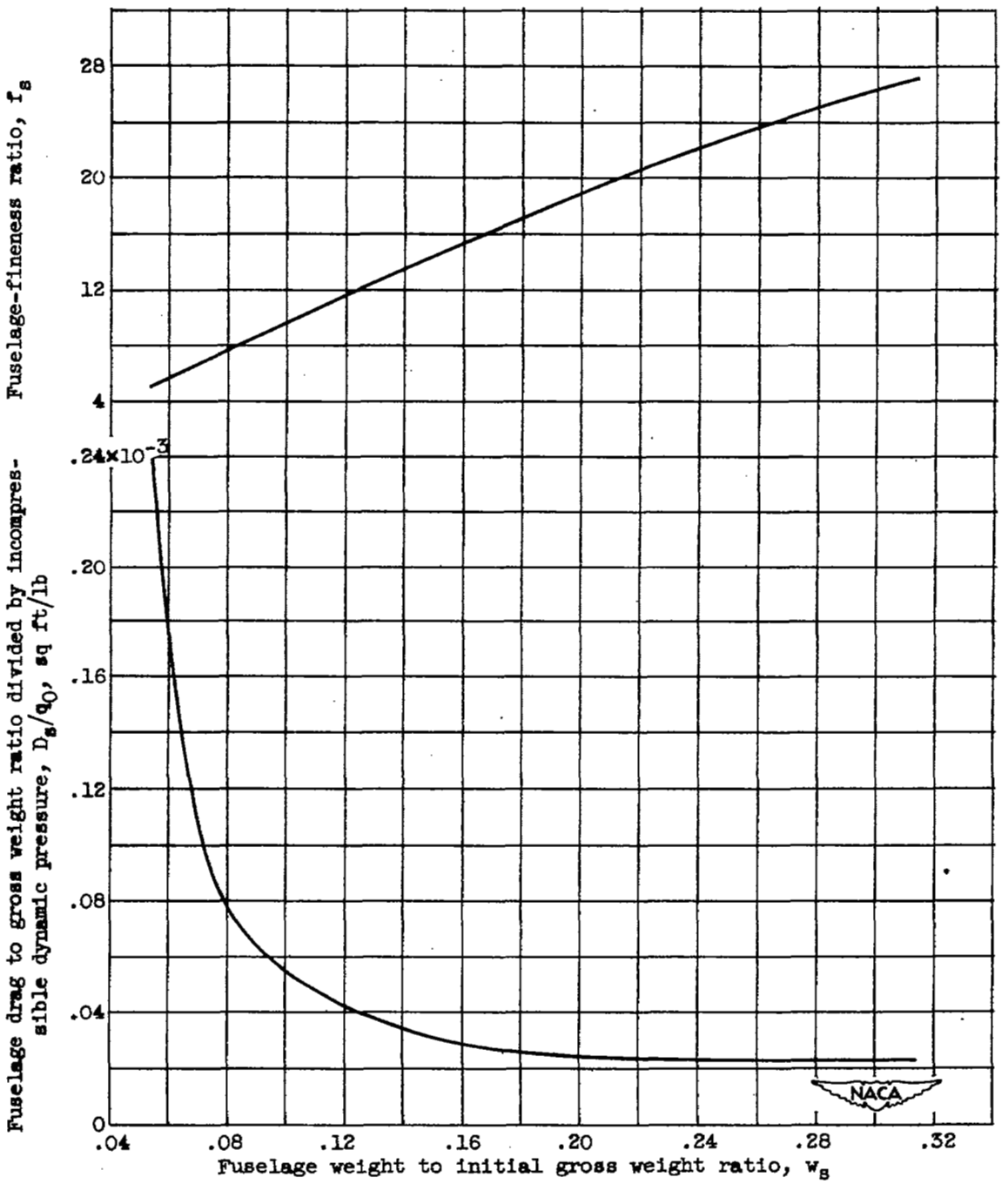

Figure 7. - Typical fuselage characteristics. Altitude, 70,000 feet; Mach number, 3.5; initial gross weight, 150,000 pounds; fuel weight to initial gross weight ratio, 0.65; fuel density, 50 pounds per cubic foot.

[redacted]